



CHORUS

This is the accepted manuscript made available via CHORUS. The article has been published as:

Nonperturbative solution of scalar Yukawa model in two- and three-body Fock space truncations

Vladimir A. Karmanov, Yang Li, Alexander V. Smirnov, and James P. Vary

Phys. Rev. D **94**, 096008 — Published 17 November 2016

DOI: [10.1103/PhysRevD.94.096008](https://doi.org/10.1103/PhysRevD.94.096008)

Nonperturbative solution of scalar Yukawa model in two- and three-body Fock space truncations

Vladimir A. Karmanov,¹ Yang Li,^{2,*} Alexander V. Smirnov,³ and James P. Vary²

¹*Lebedev Physical Institute, Leninsky Prospekt 53, 119991 Moscow, Russia*

²*Department of Physics and Astronomy, Iowa State University, Ames, IA 50011, USA*

³*JSC All-Russian Research Institute for Nuclear Power Plant Operations, 25 Ferganskaya St., 109507 Moscow, Russia*

The Light-Front Tamm-Dancoff method of finding the nonperturbative solutions in field theory is based on the Fock decomposition of the state vector, complemented with the sector-dependent nonperturbative renormalization scheme. We show in detail how to implement the renormalization procedure and to solve the simplest nontrivial example of the scalar Yukawa model in the two- and three-body Fock space truncations incorporating scalar “nucleon” and one or two scalar “pions”.

I. INTRODUCTION

Light-Front Tamm-Dancoff method is a promising nonperturbative Hamiltonian approach to quantum field theories [1]. It is based on the Fock decomposition of the state vector, which schematically reads

$$\phi(p) = \psi_1 |1\rangle + \psi_2 |2\rangle + \psi_3 |3\rangle + \dots, \quad (1)$$

where p is the total four-momentum of the physical system considered, $|n\rangle$ represents a state with the fixed number n of particles (the n -body Fock sector, $n = 1, 2, 3, \dots$), and the coefficients ψ_n are relativistic wave functions (or Fock components). The interaction between constituents, generally speaking, does not conserve the number and type of particles, so that the state vector is a mixture of an infinite number of Fock sectors. Light-Front Dynamics (LFD) proposed by Dirac [2] represents an effective formalism to calculate state vectors in Fock space. LFD defines the state vector on a null plane, also known as a light front. In covariant notations, this plane is given by the equation $\omega \cdot x = 0$, where ω is a null four-vector, $\omega^2 = 0$ (see, e.g., Ref. [3] for a review). It is traditional to choose the light front to be $x^+ \equiv t + z = 0$, corresponding to $\omega = (1, 0, 0, -1)$ [4, 5]. The state vector of a physical particle can be obtained by diagonalizing the light-front Hamilton operator which is the minus-component of the four-momentum operator:

$$\hat{P}^- \phi(p) = p^- \phi(p). \quad (2)$$

The symbol “hat” hereafter indicates that the corresponding quantity is an operator. The standard LFD minus-, plus-, and transverse components of the four-momentum are, respectively, $p^- \equiv p^0 - p^3 = (p_\perp^2 + M^2)/p^+$, $p^+ \equiv p^0 + p^3$, $\mathbf{p}_\perp \equiv (p^1, p^2)$, and M is the mass of the physical system considered. The eigenvector $\phi(p)$ can be used to calculate observables, such, e.g., as the electromagnetic form factors. The light-front Tamm-Dancoff method does not rely on the expansion in powers of coupling constants and thus is nonperturbative in nature. Wave functions obtained in this process provide direct information on the structure of the system [3]. The light-front Hamiltonian approach also enjoys some other advantages that makes it particularly appealing as an alternative method to nonperturbative Lagrangian approaches such as Lattice gauge theory [4].

In practical calculations however one can not retain the whole (infinite) set of the Fock sectors and one has to truncate the Fock decomposition of the state vector by omitting Fock sectors which contain more than a finite number N of constituents. We will refer to such an approximation as the Fock space truncation of order N , or, equivalently, the N -body truncation. In truncated Fock space, the Hamiltonian eigenvalue equation (2) reduces to a finite system of coupled linear integral equations for the wave functions $\psi_1, \psi_2, \dots, \psi_N$. It is convenient to represent this equation in a diagrammatic form by using the LFD graph techniques [3]. Fock space truncation means that one should neglect all diagrams containing more than N particles in intermediate states.

Quantum field theory suffers from divergences, with no exception for LFD. As a consequence, they appear in the eigenvalue problem Eq. (2) as well. Regularization and renormalization have to be carried out wherein the bare

* leeyoung@iastate.edu

37 coupling and bare masses, or the corresponding counterterms, are fixed via the physical coupling and physical masses.
 38 The divergences are then absorbed into the counterterms which are not observable. In nonperturbative approaches
 39 such as the light-front Tamm-Dancoff method, the renormalization, of course, is also nonperturbative. A particular
 40 challenge faced in the light-front Tamm-Dancoff method is how to guarantee the exact cancellation of the divergences.
 41 In perturbation theory, the divergences are canceled order-by-order in the coupling constant g . If some perturbative
 42 diagrams of a certain order are absent, the cancellation of divergences of that order may be destroyed. Such a situation
 43 takes place, when calculating the state vector in truncated Fock space. Indeed, the light-front Tamm-Dancoff method
 44 sums over an infinite number of diagrams with no more than N intermediate particles, while all diagrams with $(N+1)$
 45 and more intermediate particles are omitted. Consider the perturbative expansion of any calculated observable. Since
 46 the light-front Tamm-Dancoff method is nonperturbative, this expansion contains contributions of all orders in g but
 47 not an exhaustive set in a given order (say, in the order n). The contributions of the order g^n corresponding to $(N+1)$
 48 and more intermediate particles are absent because of truncation (do not confuse here the order n of perturbative
 49 expansion with the Fock space truncation of the order N). Starting with some finite order n of perturbative expansion,
 50 we would see that divergences are not canceled, because a part of the divergent contributions related to the omitted
 51 diagrams is missed. The reason is that diagrams which are of the same order in g may correspond to different
 52 Fock sectors. Since higher Fock sectors are excluded from consideration, we inevitably omit a part of (divergent)
 53 contributions needed to cancel those coming from the Fock sectors involved. As a consequence, the cancellation of
 54 divergences may not occur when following the standard renormalization procedure.

55 Fock sector-dependent renormalization (FSDR) was proposed [1] and systematically developed [6] to address this
 56 issue. While in perturbation theory the counterterms are determined order-by-order in the coupling constant, in
 57 the FSDR scheme the counterterms are determined sector-by-sector in Fock space expansion. That is, we first
 58 find the counterterms in the leading, e.g., two-body, Fock space truncation. They provide renormalization and
 59 cancellation of infinities in the leading Fock sector. However, they are not sufficient to cancel infinities in the three-
 60 body (next-to-leading) sector truncation, as it contains both the two- and three-body intermediate states. The
 61 three-body intermediate states require new counterterms — the three-body counterterms, which are found from the
 62 renormalization performed within the three-body Fock space truncation. The same procedure is continued in the
 63 four-body and higher order truncations.

64 Strict mathematical proof that this procedure eliminates infinities is complicated by the nonperturbative nature of
 65 the equations and does not yet exist. However, the validity of FSDR is strongly supported by numerical calculations.
 66 For instance, in Ref. [7] the FSDR scheme was applied to the coupling constant and fermion mass renormalization
 67 in the Yukawa model up to the three-body (one fermion plus two scalar bosons) truncation. Numerical calculations
 68 of renormalized observables demonstrated their good stability with the increase of the regularization parameters —
 69 the Pauli-Villars (PV) masses. In Refs. [8, 9], very good stability of calculated observables was found in the scalar
 70 Yukawa model up to the four-body truncation (one heavy scalar boson plus three light scalar bosons). These highly
 71 nontrivial numerical calculations provide good arguments in favor of FSDR as an effective method of nonperturbative
 72 renormalization and show a prospect for a broader range of its applications.

73 Recent studies of the scalar Yukawa model [8, 9] also give one more dimension of support for the light-front
 74 Tamm-Dancoff method equipped with the FSDR scheme. Comparison of the electromagnetic form factors obtained
 75 successively within two-, three-, and four-body truncations shows their rather fast convergence with respect to the
 76 order of truncation. This result indicates that, at least in the given model, the four-body truncation almost saturates
 77 the state vector and the calculated value of the electromagnetic form factor is already close to the exact one.

78 Originally, the FSDR scheme was formulated on the basis of the “true” Yukawa model with a spin-1/2 fermion [6].
 79 Meanwhile, renormalization of a theory of particles with spin in LFD encounters many technical difficulties having no
 80 direct relation to FSDR (more complicated spin structure of wave functions, appearance of additional counterterms
 81 depending on the light front orientation, sensitivity of results to the choice of regularization, etc.) The complexity of
 82 attendant mathematical derivations conceals, to some extent, the basic ideas of FSDR, which are rather general and
 83 applicable to a variety of realistic quantum field theories. For this reason, in the present paper we give a detailed
 84 exposition how to apply FSDR scheme in practice, using the scalar Yukawa model in truncated Fock space. This
 85 allows us to illustrate the FSDR method in a simple but nontrivial example. We will present in detail the solution of
 86 the scalar Yukawa model in the two- and three-body truncations. Another purpose of the paper concerns the following.
 87 According to the FSDR scheme, in recent studies of the scalar Yukawa model [8, 9] in the four-body truncation, the
 88 values of the bare coupling constant and the heavy boson mass counterterm from the three-body truncation were
 89 used. However, the details of their derivation were omitted. This paper serves to fill the gap. The bare coupling
 90 constant and the mass counterterm obtained below can also be used in the future for solving a relativistic bound state
 91 problem up to four-body truncation (two heavy plus two light scalar bosons).

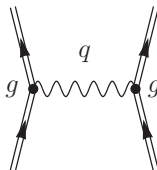


FIG. 1. Amplitude of elastic scattering of two scalar nucleons (double solid lines) near the scalar pion (wavy line) pole $q^2 = \mu^2$. In the vicinity of this pole the amplitude has the form $\mathcal{M}_{\chi\chi \rightarrow \chi\chi} = -g^2/(q^2 - \mu^2 + i0)$.

92 Note that the renormalized scalar Yukawa model in the three-body truncation was also studied in Ref. [10], but
 93 without reference to FSDR. Though such an approach led to acceptable results for the particular model and the
 94 particular order of truncation, it does not seem universal from the point of view of divergence cancellation, in contrast
 95 to FSDR.

96 The paper is organized as follows. We start in Sec. II with a brief description of the scalar Yukawa model. In
 97 Sec. III a general equation for the state vector in LFD is formulated. In Sec. IV we expose the main features of FSDR.
 98 Solutions for the state vector in the scalar Yukawa model are found in the two- and three-body truncations in Secs. V
 99 and VI, respectively. In Sec. VII we calculate an observable quantity — the scalar heavy boson electromagnetic form
 100 factor — in the two- and three-body truncations, successively. In Sec. VIII we discuss the properties of the bare
 101 coupling constant determined by the renormalization. Sec. IX contains concluding remarks.

102

II. SCALAR YUKAWA MODEL

103 We consider an electrically charged heavy scalar boson (χ) with the physical mass m , dressed by lighter neutral
 104 scalar bosons (φ) with the physical mass μ . To mimic somehow real nucleon-pion physics, we tentatively assign them,
 105 respectively, the nucleon and pion masses¹, $m = 0.94$, $\mu = 0.14$, and will call them scalar nucleon and scalar pion,
 106 omitting sometimes the word “scalar”, for shortness. The corresponding Lagrangian reads

$$\mathcal{L} = \partial_\nu \chi^\dagger \partial^\nu \chi - m^2 \chi^\dagger \chi + \frac{1}{2} \partial_\nu \varphi \partial^\nu \varphi - \frac{1}{2} \mu^2 \varphi^2 + g_0 \chi^\dagger \chi \varphi + \delta m^2 \chi^\dagger \chi, \quad (3)$$

107 where the bare coupling constant g_0 and the nucleon mass counterterm δm^2 are renormalization constants to be
 108 determined by the renormalization procedure. We denote the physical coupling constant as g which is found from
 109 typical scattering experiments, e.g., by the analytic continuation of the measured two scalar nucleon elastic scattering
 110 amplitude, as a function of the momentum transfer square, to the scalar pion pole in the nonphysical kinematical
 112 region (see Fig. 1). For convenience, we introduce a dimensionless coupling constant

$$\alpha \equiv \frac{g^2}{16\pi m^2}, \quad (4)$$

113 which appears as the coupling constant of the nonrelativistic Yukawa potential $U(r) = -\alpha e^{-\mu r}/r$ between two scalar
 114 nucleons. The electromagnetic interaction is not explicitly included into the Lagrangian (3) because it is assumed much
 115 weaker than the interaction between scalar nucleons and pions. We will need it only for the calculation of the nucleon
 116 electromagnetic form factor, where it will be taken into account perturbatively. In contrast to the electromagnetic
 117 fine structure constant e^2 , the coupling constant α is not implied to be small and no expansions in it are used.

118 To regularize the theory, we introduce a PV scalar pion field φ_{PV} with a large mass $\mu_{\text{PV}} \gg m, \mu$. The PV pion field
 119 is enough to regularize rather weak (logarithmic) divergences which appear in the scalar Yukawa model, i.e., there is
 120 no need to introduce an analogous PV nucleon field. Since PV fields have negative metric, the Lagrangian becomes

$$\mathcal{L} = \partial_\nu \chi^\dagger \partial^\nu \chi - m^2 \chi^\dagger \chi + \delta m^2 \chi^\dagger \chi + \frac{1}{2} \sum_{j=0}^1 (-1)^j [\partial_\nu \varphi_j \partial^\nu \varphi_j - \mu_j^2 \varphi_j^2] + \sum_{j=0}^1 g_0 \chi^\dagger \chi \varphi_j, \quad (5)$$

¹ The masses are in GeV. However in this model, only the ratio μ/m matters, and we will suppress all units.

where the index j denotes a type of particle: the values $j = 0$ and $j = 1$ correspond, respectively, to the physical and PV scalar pion fields, $\mu_0 \equiv \mu$, $\mu_1 \equiv \mu_{\text{PV}}$. Similar procedure was used in Ref. [11].

Our main goal is to calculate the state vector $\phi(p)$ of the scalar nucleon. Then it can be used for calculating observables. The Fock space generated by the Lagrangian (3) embraces all Fock sectors composed of scalar nucleons, antinucleons, and pions. Each Fock sector contains one nucleon plus an arbitrary number of nucleon-antinucleon pairs plus arbitrary number of pions. It is known however that the contribution from the nucleon-antinucleon loops causes the instability of the vacuum [12, 13]. We therefore truncate away all Fock sectors with antinucleons and construct a truncated Fock space from a set of Fock sectors with one scalar nucleon and increasing number of scalar pions. This procedure, however, comes with a penalty, as we will discuss below.

The introduction of PV scalar pions into the Lagrangian (5) extends the Fock space, which impacts the rule of particle counting inside Fock sectors. We postulate that PV scalar pions come to the theory on equal grounds with the physical ones. This means that any pion is counted as one particle, regardless to its type.

III. STATE VECTOR IN LIGHT-FRONT DYNAMICS

The explicitly covariant form of LFD, as a more general approach mentioned in the Introduction, has many technical advantages in comparison with its noncovariant forms [3]. In particular, the four-vector ω serves as an indicator of possible dependence of calculated results on the light front orientation. This is especially important in approximate nonperturbative calculations, where such dependence may appear in calculated observables due to rotational symmetry breaking. For particles with spin, covariant LFD facilitates studying the spin structure of scattering amplitudes. In spite of these merits, for the case of scalar particles, these different forms of LFD are almost equivalent, even from the technical point of view. For this reason, we will not distinguish them below and, retaining in some instances the four-vector ω in explicit form, we will assume that it has definite components $(1, 0, 0, -1)$. If so, we have $\omega^+ = 0$, $\omega_{\perp} = \mathbf{0}$, $\omega^- = 2$, and $\omega \cdot a = a^+$ for an arbitrary four-vector a .

In LFD the state vector of a physical state is a solution of the eigenvalue equation (2) which can be written in an invariant form:

$$\hat{P}^2 \phi(p) = M^2 \phi(p), \quad (6)$$

where $\hat{P}^2 = \hat{P}^+ \hat{P}^- - \hat{P}_{\perp}^2$. The plus- and transverse components of the momentum operator in LFD do not contain the interaction; so they can be substituted, respectively, by the p^+ and \mathbf{p}_{\perp} components of the total four-momentum p . The interaction is only contained in the minus-component of the momentum operator which can be represented as a sum of the free and interacting parts: $\hat{P}^- = \hat{P}_0^- + \hat{P}_{\text{int}}^-$. The interacting part, in its turn, tightly relates to the light-front interaction Hamiltonian $\mathcal{H}_{\text{int}}(x)$:

$$\hat{P}_{\text{int}}^- = 2 \int \mathcal{H}_{\text{int}}(x) \delta(\omega \cdot x) d^4x = 2 \int_{-\infty}^{+\infty} \tilde{\mathcal{H}}_{\text{int}}(\omega\tau) \frac{d\tau}{2\pi}, \quad (7)$$

where $\tilde{\mathcal{H}}_{\text{int}}$ is a Fourier transform of the interaction Hamiltonian:

$$\tilde{\mathcal{H}}_{\text{int}}(\omega\tau) = \int \mathcal{H}_{\text{int}}(x) e^{-i(\omega \cdot x)\tau} d^4x. \quad (8)$$

In covariant form, the four-momentum operator can be written as

$$\hat{P}^{\nu} = \hat{P}_0^{\nu} + \omega^{\nu} \int_{-\infty}^{+\infty} \tilde{\mathcal{H}}_{\text{int}}(\omega\tau) \frac{d\tau}{2\pi}. \quad (9)$$

Since $\omega^2 = 0$, we have $\omega \cdot \hat{P} = \omega \cdot \hat{P}_0 = p^+$. In Ref. [10] it was proven that the operators $\omega \cdot \hat{P}_0$ and \hat{P}_{int}^- commute. We thus get

$$\hat{P}^2 = \hat{P}_0^2 + 2p^+ \int_{-\infty}^{+\infty} \tilde{\mathcal{H}}_{\text{int}}(\omega\tau) \frac{d\tau}{2\pi}. \quad (10)$$

Substituting this result into Eq. (6), we finally obtain [10]

$$\left[\hat{P}_0^2 - M^2 \right] \phi(p) = -2p^+ \int_{-\infty}^{+\infty} \tilde{\mathcal{H}}_{\text{int}}(\omega\tau) \frac{d\tau}{2\pi} \phi(p). \quad (11)$$

155 The interaction Hamiltonian can be derived from the corresponding Lagrangian. We need the Hamiltonian in the
 156 interaction representation, i.e., that expressed through the free fields. For particles with spin or if the interaction
 157 depends on field derivatives the procedure may be, generally speaking, very nontrivial. The reason is that in LFD
 158 some of the equations of motion for field components are not dynamical equations but constraints. Exclusion of the
 159 non-dynamical degrees of freedom give rise to specific (contact) terms in the Hamiltonian. This point is explained
 160 in more detail in Ref. [14]. Fortunately, all that does not concern the case of scalar Yukawa model we consider here,
 161 because each scalar field has only one component. If so, one can simply identify the Hamiltonian with the interaction
 162 part of the Lagrangian taken with the opposite sign:

$$\mathcal{H}_{\text{int}}(x) = -g_0 \chi^\dagger \chi \varphi - \delta m^2 \chi^\dagger \chi. \quad (12)$$

163 To avoid overload with notations, we do not show explicitly the contribution of PV particles. They can be introduced
 164 later directly in the equations for the Fock components.

165 To solve Eq. (11), we make use of the Fock decomposition of the state vector $\phi(p)$, as given schematically by Eq. (1).
 166 We define the n -body Fock sector as a state containing one free scalar nucleon with the four-momentum k_1 plus $(n-1)$
 167 free scalar pions with the four-momenta k_2, \dots, k_n . This state is obtained by acting with the corresponding creation
 168 operators on the vacuum:

$$|n\rangle = \hat{a}^\dagger(\mathbf{k}_1) \hat{c}^\dagger(\mathbf{k}_2) \dots \hat{c}^\dagger(\mathbf{k}_n) |0\rangle. \quad (13)$$

169 The creation operators satisfy the standard commutation relation $[\hat{a}(\mathbf{k}), \hat{a}^\dagger(\mathbf{k}')] = \delta^{(3)}(\mathbf{k} - \mathbf{k}')$ (for \hat{c} and \hat{c}^\dagger analo-
 170 gously). Due to the interaction, the total four-momentum p of the physical nucleon is not equal to the sum of the
 171 constituent four-momenta: $k_1 + \dots + k_n \neq p$, i.e., momentum conservation is violated. Within LFD, only plus- and
 172 transverse components of the total four-momentum are conserved:

$$k_1^+ + \dots + k_n^+ = p^+, \quad \mathbf{k}_{1\perp} + \dots + \mathbf{k}_{n\perp} = \mathbf{p}_\perp. \quad (14)$$

173 In the following, we will set $\mathbf{p}_\perp = \mathbf{0}$. This can be safely done due to the invariance of LFD with respect to transverse
 174 boosts. Using the four-vector ω introduced above, the relations (14) can be written in an explicitly covariant form
 175 which looks like the momentum conservation law:

$$k_1 + \dots + k_n = p + \omega \tau_n. \quad (15)$$

176 The scalar parameter τ_n (the off-shell light-front energy) can be expressed through the particle momenta by squaring
 177 both sides of Eq. (15):

$$\tau_n = \frac{s_n - M^2}{2p^+}, \quad (16)$$

178 where s_n is the invariant mass squared of the n -body Fock sector:

$$s_n \equiv (k_1 + \dots + k_n)^2. \quad (17)$$

179 By definition, $s_1 = m^2$. Note that s_n is an eigenvalue of the free four-momentum operator squared $\hat{P}_0^2 = p^+ \hat{P}_0^- - p_\perp^2$:

$$\hat{P}_0^2 |n\rangle = s_n |n\rangle. \quad (18)$$

180 The Fock decomposition of the physical scalar nucleon state vector can be written as [10]:

$$\phi(p) = \sum_{n=1}^{\infty} \frac{2p^+ (2\pi)^{3/2}}{(n-1)!} \int d\tau_n \left(\prod_{i=1}^n \frac{d^3 k_i}{(2\pi)^{3/2} \sqrt{2\varepsilon_{k_i}}} \right) \psi_n(k_1, \dots, k_n; p) \delta^{(4)}(k_1 + \dots + k_n - p - \omega \tau_n) |n\rangle, \quad (19)$$

181 where $\varepsilon_{k_i} = \sqrt{\mathbf{k}_i^2 + m_i^2}$ and m_i is the mass of the i -th constituent. All the four-momenta are on their mass shells,
 182 $k_i^2 = m_i^2$. The combinatorial factor $1/(n-1)!$ takes into account the identity of scalar pions. The Dirac's delta-
 183 function accounts for the four-momentum conservation law (15). Note that Eq. (19) may be considered as an exact
 184 definition of the light-front wave functions ψ_n .

185 The state vector satisfies the normalization condition

$$\phi^\dagger(p') \phi(p) = 2\varepsilon_p \delta^{(3)}(\mathbf{p} - \mathbf{p}') \quad (20)$$

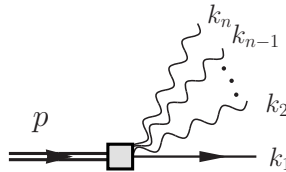


FIG. 2. Diagram for the n -body vertex function $\Gamma_n(k_1, k_2, \dots, k_n; p)$. The scalar pions are represented by the wavy lines. The constituent and physical scalar nucleons are represented by the single and double straight lines, respectively.

186 which reduces to

$$\sum_{n=1}^{\infty} I_n = 1, \quad (21)$$

187 where

$$I_n = \frac{2p^+}{(2\pi)^{3(n-1)}(n-1)!} \int d\tau_n \left(\prod_{i=1}^n \frac{d^3 k_i}{2\varepsilon_{k_i}} \right) |\psi_n(k_1, \dots, k_n; p)|^2 \delta^{(4)}(k_1 + \dots + k_n - p - \omega\tau_n) \quad (22)$$

188 is the n -body Fock sector contribution to the full norm equal to unity. By its physical sense, I_n is the probability
189 that the physical state appears in the n -body Fock sector.

190 It is useful to introduce the light-front vertex functions Γ_n related to the wave functions by

$$\Gamma_n \equiv (s_n - M^2)\psi_n \quad (23)$$

191 and the new state vector

$$\mathcal{G}(p) = 2p^+ \hat{\tau} \phi(p), \quad (24)$$

192 where the operator $\hat{\tau}$ acting on each Fock component ψ_n yields $\tau_n \psi_n$. $\mathcal{G}(p)$ has the same Fock decomposition (19),
193 changing the wave functions ψ_n by the corresponding vertex functions Γ_n . Using Eqs. (18) and (16), and the defini-
194 tion (23), the main dynamical equation (11) for the state vector can be rewritten as [10]

$$\mathcal{G}(p) = \frac{1}{2\pi} \int_{-\infty}^{+\infty} \left[-\tilde{\mathcal{H}}_{\text{int}}(\omega\tau) \right] \frac{d\tau}{\tau} \mathcal{G}(p). \quad (25)$$

195 The vertex function Γ_n is closely related to the full transition amplitude [11]. This connection allows us to represent
196 the system of equations for the vertex functions using the light-front time-ordered diagrams via the so-called covariant
197 LFD graphical rules [3]. An n -body vertex diagram is shown in Fig. 2.

198 For practical applications, it is convenient to transform the dependence of the wave and vertex functions on the con-
199 stituent four-momenta k_1, \dots, k_n into their dependence on the light-front variables which are the transverse momenta
200 $\mathbf{k}_{i\perp}$ and the longitudinal momentum fractions $x_i \equiv k_i^+ / p^+$ ($i = 1, \dots, n$). The n pairs of the arguments $(\mathbf{k}_{i\perp}, x_i)$ are
201 constrained by the conditions
202

$$\sum_{i=1}^n x_i = 1, \quad \sum_{i=1}^n \mathbf{k}_{i\perp} = \mathbf{0}, \quad (26)$$

203 directly following from Eqs. (14). We thus have $(n-1)$ pairs of independent kinematical variables $(\mathbf{k}_{i\perp}, x_i)$ in the
204 n -body Fock sector. The invariant mass squared s_n of the n -body Fock sector is expressed through the light-front
205 variables as

$$s_n = \sum_{i=1}^n \frac{k_{i\perp}^2 + m_i^2}{x_i}. \quad (27)$$

206 The dependence of the wave and vertex functions on the total four-momentum p reduces to their dependence on
207 $p^2 = M^2$. It is convenient to exclude, by means of Eqs. (26), the scalar nucleon momenta $\mathbf{k}_{1\perp}$ and x_1 and to choose
208 the scalar pion momenta as a set of independent variables. We thus write

$$\Gamma_n = \Gamma_n(\mathbf{k}_{2\perp}, x_2, \dots, \mathbf{k}_{n\perp}, x_n; M^2) \quad (28)$$

209 and analogously for ψ_n . For simplicity, we will further suppress the dependence of Fock components on M^2 for the
210 physical particle ($M^2 = m^2$), whenever there is no danger of confusion.

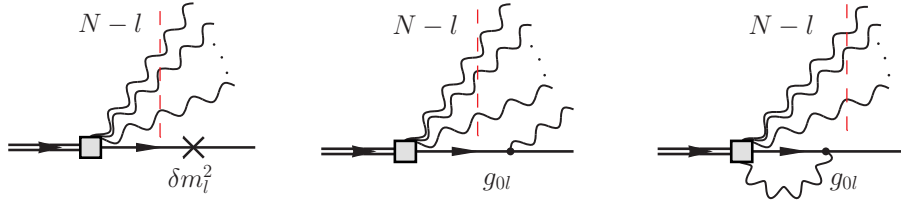


FIG. 3. Assignment of Fock sector dependent bare parameters. Here N is the maximal number of particles allowed by the truncation [one scalar nucleon plus $(N - 1)$ scalar pions] and $N - l$ is the number of pion spectators which are intersected by the dashed line.

211

IV. FOCK SECTOR DEPENDENT RENORMALIZATION

Fock sector dependent renormalization (FSDR) is a systematic scheme to renormalize light-front Hamiltonian field theory in truncated Fock space [6]. In this approach, the bare parameters (i.e., the full set of parameters entering into the interaction Hamiltonian and used for renormalization, such as bare coupling constants, bare masses, various counterterms, etc.) explicitly depend on the Fock sector, where they appear in the equations for the Fock components. For example, instead of the unique bare coupling constant g_0 one should assign to each interaction vertex in light-front diagrams the factor g_{0l} , where the index l equals the difference between the order of Fock space truncation N and the total number of other particles “in flight” at the instant which corresponds to the given vertex. The same concerns the mass counterterm δm^2 . Actually, one has to deal with a whole series of bare coupling constants and mass counterterms being different for different Fock sectors:

$$g_0 \rightarrow g_{0l}, \quad \delta m^2 \rightarrow \delta m_l^2, \quad (l = 1, 2, \dots, N). \quad (29)$$

In the general case, $l = (N - n_s)$, where n_s is the number of pion spectators. The assignment of the Fock sector dependence is illustrated in Fig. 3.

These sector dependent bare parameters can be determined successively, by increasing the order of truncation N . The trivial case $N = 1$ yields $g_{01} = 0$ and $\delta m_1^2 = 0$, since the only particle allowed is the scalar nucleon with no interactions and mass renormalization. Then, g_{02} and δm_2^2 are determined in the two-body truncation ($N = 2$), where the state vector is a superposition of the single scalar nucleon and one scalar nucleon plus one scalar pion Fock sectors. g_{03} and δm_3^2 are determined in the three-body ($N = 3$) truncation, where the scalar nucleon plus two scalar pions Fock sector is added. The bare parameters g_{02} and δm_2^2 appearing in this approximation as well are used untouched, as they have been found from the $N = 2$ case. The process repeats, until one’s desired Fock sector truncation is reached. Therefore, in order to find the state vector for the N -body truncation, one has to solve first the two-, three-, ..., $(N - 1)$ -body problems. Below, to distinguish from each other the same quantities calculated in different approximations, we will supply the former ones by the superscript “ (N) ” indicating the order of Fock space truncation. Thus $\Gamma_n^{(N)}$ means the n -body vertex function found within the N -body Fock space truncation, $I_n^{(N)}$ stands for the n -body Fock sector norm obtained in the same approximation, etc.

The bare parameters relate to the physical ones by the renormalization conditions. The scalar nucleon mass counterterm is determined from the requirement that the physical and constituent nucleon masses coincide, i.e., $M = m$. In other words, one demands that the interaction does not change the nucleon mass. The bare coupling constant is obtained from the standard condition that the “dressed” two-body on-energy-shell vertex function turns into the physical coupling constant (see, e.g., Ref. [15]):

$$\sqrt{Z_\chi} \tilde{\Gamma}_2^{\text{on-shell}} \sqrt{Z_\chi} \sqrt{Z_\varphi} = g, \quad (30)$$

where Z ’s are the so-called field strength renormalization factors taking into account “radiative” corrections to the two-body vertex external legs and $\tilde{\Gamma}$ denotes the two-body vertex amputated from all radiative corrections to its external legs. The factor Z_χ tightly relates to the corresponding scalar nucleon self-energy $\Sigma(p^2)$ by

$$Z_\chi = [1 - \Sigma'(m^2)]^{-1}, \quad (31)$$

where the prime means the derivative

$$\Sigma'(m^2) \equiv \left. \frac{\partial}{\partial p^2} \Sigma(p^2) \right|_{p^2=m^2}. \quad (32)$$

245 The self-energy is given by a sum of amplitudes of all irreducible diagrams with one-body initial and final states. For
246 the scalar pion factor Z_φ a formula analogous to Eq. (31) can be written down.

247 Note that the factorization of the “dressed” vertex into a product of the “bare” vertex $\tilde{\Gamma}_2$ and the external leg
248 factors \sqrt{Z} ’s, which appears automatically in the four-dimensional Feynman approach, is a very nontrivial fact in the
249 framework of LFD. First, such a factorization in LFD takes place on the energy shell only, while in the Feynman case
250 it holds for the off-mass-shell vertex as well. Second, the factorization may be destroyed by approximations, e.g., the
251 Fock space truncation. Fortunately, the LFD two-body vertex function enters into the renormalization condition (30)
252 just being taken on the energy shell, where it coincides with the corresponding Feynman on-mass-shell two-body
253 vertex. In addition, we do not consider here antinucleon contributions to the state vector, that leaves scalar pion
254 a point-like particle, so that $Z_\varphi \equiv 1$. Under these conditions, one can safely accept Eq. (30) as a starting point
255 of the bare coupling constant renormalization, even in truncated Fock space. Below we relate $\tilde{\Gamma}_2$ to the previously
256 introduced two-body vertex function Γ_2 .

257 The condition that the nucleon-pion state is on the energy shell means that the constituent four-momenta satisfy
258 the conservation law $k_1 + k_2 = p$ and, hence, $s_2 = (k_1 + k_2)^2 = m^2$. Going over to the light-front variables, we have
259 $x_1 + x_2 = 1$ and $\mathbf{k}_{1\perp} + \mathbf{k}_{2\perp} = \mathbf{0}$. So, the two-body vertex function depends on the two variables which we denote as

$$k_\perp \equiv |\mathbf{k}_{2\perp}| = |\mathbf{k}_{1\perp}|, \quad x \equiv x_2 = 1 - x_1. \quad (33)$$

260 The invariant two-body mass squared in terms of these variables has the form

$$s_2 = \frac{k_\perp^2 + \mu^2}{x} + \frac{k_\perp^2 + m^2}{1 - x}. \quad (34)$$

261 On the energy shell, where $s_2 = m^2$, we get

$$k_\perp = k_\perp^*(x) \equiv i\sqrt{m^2 x^2 + \mu^2(1 - x)} \quad (35)$$

262 (the choice of the sign, $+i\sqrt{\dots}$ or $-i\sqrt{\dots}$, is not important, since the two-body vertex function depends in fact on
263 k_\perp^2) and

$$\tilde{\Gamma}_2^{\text{on-shell}} = \tilde{\Gamma}_2(s_2 = m^2) = \tilde{\Gamma}_2(k_\perp^*(x), x). \quad (36)$$

264 Since the field strength renormalization factors are constants (i.e., they do not depend on any kinematical variables),
265 the renormalization condition (30) implies that the two-body vertex function taken on the energy shell must turn into
266 a constant too. This is indeed so in perturbation theory. It would be true in exact nonperturbative calculations, if they
267 were possible. In approximate nonperturbative approach however such a property is not automatically guaranteed
268 and the calculated two-body vertex keeps x -dependence even on the energy shell. If so, one may consider Eq. (30)
269 to be true for some particular value of $x = x^*$ only, choosing x^* at our own will [16, 17]. An evident flaw here is the
270 dependence of calculated observables on the extra nonphysical parameter x^* . Since there are not any strict arguments
271 in favor of some preset value x^* , whether this dependence is weak or not is a matter of chance. An alternative way
272 proposed in Ref. [7] seems more justified. It demands Eq. (30) to be true *for all* $0 \leq x \leq 1$, but admits x -dependence
273 of the bare parameters, uniquely determined directly from the system of equations for the Fock components. Now
274 the nonphysical dependence of the on-energy-shell two-body vertex function on kinematical variables, caused by the
275 Fock space truncation, shifts to unobserved quantities, while the renormalization condition (30) becomes fully self-
276 consistent. One may also expect that this method improves the stability of calculated observables as a function of the
277 regularization parameters (PV masses), as, e.g., the calculations of the spin-1/2 fermion anomalous magnetic moment
278 in the Yukawa model, obtained in Ref. [7], show.

279 We emphasize: by making a truncation, we approximate the initial field-theoretical Hamiltonian by a matrix of
280 finite dimension (in terms of the particle number), acting in Fock space. This is the reason, why in “new” dynamics
281 the on-shell two-body vertex function (36) calculated with constant bare parameters acquires dependence on the
282 variable x . Assuming appropriate x -dependence of the bare coupling constant which implicitly enters into $\tilde{\Gamma}_2^{\text{on-shell}}$
283 allows the latter to be x -independent. So, x -dependence of bare parameters compensates, to some extent, the effect
284 of missed (because of the Fock space truncation) contributions. In Sec. VIII below, by using an example, we will
285 demonstrate explicitly that after taking into account the contribution eliminated by truncation the x -dependence of
286 the on-shell two-body vertex function does completely disappear.

287 Upon adoption within a truncated Fock space, the general renormalization condition (30) should be reformulated
288 according to the FSDR requirements. The factor $\sqrt{Z_\chi}$ in front of $\tilde{\Gamma}_2^{\text{on-shell}}$ comes from the “dressing” of a single

289 scalar nucleon line. For the Fock space truncation of order N it should be thus substituted by $\sqrt{Z_\chi^{(N)}}$. The analogous
 290 factor behind $\tilde{\Gamma}_2^{\text{on-shell}}$ corresponds to the “dressing” of a scalar nucleon line in the two-body (nucleon plus pion) state.
 291 Since the total number of particles in any Fock sector can not exceed N , this factor should be calculated in the lower
 292 $(N - 1)$ approximation. Taking into account that $\sqrt{Z_\varphi} \equiv 1$, we obtain

$$\sqrt{Z_\chi^{(N)}} \tilde{\Gamma}_2^{(N)}(s_2 = m^2) \sqrt{Z_\chi^{(N-1)}} = g. \quad (37)$$

293 To make practical use of Eq. (37) one should relate the “amputated” two-body vertex $\tilde{\Gamma}_2$ to the previously introduced
 294 two-body Fock component Γ_2 . This relation has the form [16]²

$$\Gamma_2^{(N)}(s_2 = m^2) = \sqrt{I_1^{(N)}} \tilde{\Gamma}_2^{(N)}(s_2 = m^2) Z_\chi^{(N-1)}, \quad (38)$$

295 where $I_1^{(N)}$ is the one-body Fock sector normalization integral in the N -body truncated Fock space. Its calculation
 296 according to Eq. (22) yields $I_1^{(N)} = |\psi_1^{(N)}|^2$. Note that the normalization condition (21) for the state vector now
 297 acquires the form

$$\sum_{n=1}^N I_n^{(N)} = 1. \quad (39)$$

298 In terms of the light-front variables, $I_n^{(N)}$ is expressed through the corresponding vertex function as

$$I_n^{(N)} = \frac{2}{(2\pi)^{3(n-1)}(n-1)!} \int \prod_{i=1}^n \frac{d^2 k_{i\perp} dx_i}{2x_i} \left[\frac{\Gamma_n^{(N)}}{s_n - M^2} \right]^2 \delta^{(2)} \left(\sum_{i=1}^n \mathbf{k}_{i\perp} \right) \delta \left(\sum_{i=1}^n x_i - 1 \right). \quad (40)$$

299 In Ref. [16] it was proven that the field strength renormalization factor for a spin-1/2 fermion exactly coincides with
 300 the corresponding one-body normalization integral. The proof can be easily reduced to the scalar case. Applying this
 301 result to the quantities in truncated Fock space means

$$Z_\chi^{(N)} = I_1^{(N)}. \quad (41)$$

302 Combining Eqs. (37), (38), and (41) together gives the final form of the renormalization condition for the bare coupling
 303 constant:

$$\Gamma_2^{(N)}(s_2 = m^2) = g \sqrt{I_1^{(N-1)}}. \quad (42)$$

On introducing PV particles, one has to supply the vertex functions with additional indices pointing out the types
 of scalar pions in the corresponding Fock sectors. We will denote the pion type by the superscript j_l , $l = 2, 3, \dots, n$:

$$\Gamma_n^{(N)}(\mathbf{k}_{2\perp}, x_2, \dots, \mathbf{k}_{n\perp}, x_n) \rightarrow \Gamma_n^{(N)j_2 \dots j_n}(\mathbf{k}_{2\perp}, x_2, \dots, \mathbf{k}_{n\perp}, x_n).$$

304 According to the notations accepted in Sec. II, $j_l = 0$ stands for a physical pion, while $j_l = 1$ corresponds to a PV
 305 one. The renormalization condition (42) is imposed on the physical component $\Gamma_2^{(N)j_2=0}$ of the two-body vertex.

306 V. SCALAR NUCLEON STATE VECTOR IN THE TWO-BODY ($N = 2$) TRUNCATION

307 A. Equations for the Fock components and their solution

308 In the two-body truncation, we keep up to two particles (one scalar nucleon plus one scalar pion) in the Fock space.
 309 The system of equations for the vertex functions, obtained from the general equation (25) for the state vector, is
 310 shown graphically in Fig. 4. The rules of the LFD graph techniques are exposed, in covariant form, e.g., in Ref. [3].
 312 Applying them to the system of equations considered, one gets

² Though in Ref. [16] the Yukawa model with a spin-1/2 “nucleon” was considered, some results obtained there are rather general and can be applied to the scalar case as well.

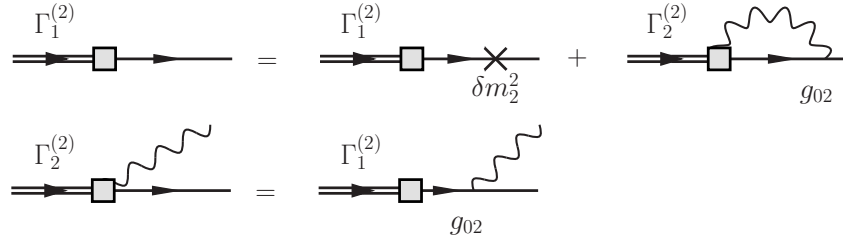


FIG. 4. System of equations for the vertex functions in the two-body truncation.

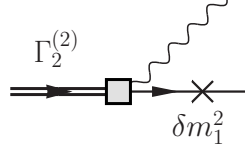


FIG. 5. Contribution from the mass counterterm, which is absent in the two-body truncation.

$$\Gamma_1^{(2)} = \delta m_2^2 \frac{\Gamma_1^{(2)}}{m^2 - M^2} + g_{02} \sum_{j=0}^1 (-1)^j \int_0^1 \frac{dx}{2x(1-x)} \int \frac{d^2 k_\perp}{(2\pi)^3} \frac{\Gamma_2^{(2)j}(k_\perp, x)}{s_2^j - M^2}, \quad (43)$$

$$\Gamma_2^{(2)j}(k_\perp, x) = g_{02} \frac{\Gamma_1^{(2)}}{m^2 - M^2}, \quad (44)$$

313 where

$$s_2^j = \frac{k_\perp^2 + \mu_j^2}{x} + \frac{k_\perp^2 + m^2}{1-x} \quad (45)$$

314 is the invariant mass squared of the two-body state made from the one scalar nucleon and one scalar pion of the
 315 j -th type [cf. with Eq. (34)]. The arguments of the two-body vertex function are defined by Eqs. (33). The factor
 316 $(-1)^j$ takes into account the negative norm of the PV scalar pion. Note that $\Gamma_1^{(2)}/(m^2 - M^2) = \psi_1^{(2)}$ is a constant in
 317 the sense that it does not depend on kinematical variables. The bare parameters are assigned to the vertices of the
 318 diagrams, according to the FSDR requirements. This is the reason why Eq. (44) does not contain, on its right-hand
 319 side, a contribution from the scalar nucleon mass counterterm. In principle, one should add such a contribution (it is
 320 shown in Fig. 5), because it is generated by the interaction Hamiltonian (12). At the same time, within the two-body
 321 truncation, one has to assign the factor δm_1^2 to the corresponding vertex given by the mass counterterm, since there
 322 is already one scalar pion in flight in the two-body state. Due to the fact that $\delta m_1^2 = 0$, the diagram in Fig. 5 does
 323 not contribute to Eq. (44).

325 In the limit $M \rightarrow m$ the one-body vertex function $\Gamma_1^{(2)} \sim (m^2 - M^2) \rightarrow 0$, while $\psi_1^{(2)}$ has a constant value determined
 326 from the normalization condition (39) for the state vector. The system of equations (43) and (44) thus reduces to

$$0 = \delta m_2^2 \psi_1^{(2)} - g_{02}^2 \bar{\Sigma}^{(2)}(m^2) \psi_1^{(2)}, \quad (46)$$

$$\Gamma_2^{(2)j}(k_\perp, x) = g_{02} \psi_1^{(2)}, \quad (47)$$

327 where $\bar{\Sigma}^{(2)}$ is nothing but the scalar nucleon self-energy in the two-body approximation, $\Sigma^{(2)}$, amputated from the
 328 coupling constant squared. For an arbitrary value of its argument p^2 , this function is given by

$$\bar{\Sigma}^{(2)}(p^2) = - \sum_{j=0}^1 (-1)^j \int_0^1 \frac{dx}{2x(1-x)} \int \frac{d^2 k_\perp}{(2\pi)^3} \frac{1}{s_2^j - p^2}. \quad (48)$$

329 By definition, $\bar{\Sigma}^{(2)}(p^2) = \Sigma^{(2)}(p^2)/g_{02}^2$. It enters into Eq. (46) at $p^2 = m^2$. When the PV scalar pion mass μ_1 tends
330 to infinity, $\bar{\Sigma}^{(2)}(p^2)$ diverges like $\log(\mu_1/m)$. The function $\bar{\Sigma}^{(2)}(p^2)$ is calculated in an explicit form in Appendix A.

331 Equation (46) determines the mass counterterm:

$$\delta m_2^2 = g_{02}^2 \bar{\Sigma}^{(2)}(m^2), \quad (49)$$

332 while $\psi_1^{(2)}$ still remains a free constant. δm_2^2 is not immediately needed for the two-body truncation and will be
333 analyzed later. The two-body vertex function, as follows from Eq. (47), is a constant too: it depends neither on
334 kinematical variables nor on the index j . This fact is a direct consequence of the two-body Fock space truncation
335 and, generally speaking, it does not hold in higher order truncations. The renormalization condition (42) at $N = 2$
336 reads simply

$$\Gamma_2^{(2)j=0}(k_\perp^*(x), x) = g, \quad (50)$$

337 where we have used $I_1^{(1)} = 1$ (free theory). Since $\Gamma_2^{(2)j}(k_\perp, x) \equiv \Gamma_2^{(2)}$ is a constant, one gets

$$\Gamma_2^{(2)} = g. \quad (51)$$

338 The one-body wave function $\psi_1^{(2)}$ is now defined by the state vector normalization:

$$\psi_1^{(2)} = \sqrt{I_1^{(2)}} = \sqrt{1 - I_2^{(2)}}, \quad (52)$$

339 where

$$\begin{aligned} I_2^{(2)} &= \sum_{j=0}^1 (-1)^j \int_0^1 \frac{dx}{2x(1-x)} \int \frac{d^2 k_\perp}{(2\pi)^3} \left[\frac{\Gamma_2^{(2)}}{s_2^j - m^2} \right]^2 \\ &= \frac{g^2}{16\pi^2 m^2} \int_0^1 dx \left[\frac{x(1-x)}{(1-x)\mu^2/m^2 + x^2} - \frac{x(1-x)}{(1-x)\mu_1^2/m^2 + x^2} \right]. \end{aligned} \quad (53)$$

340 The two-body Fock sector norm $I_2^{(2)}$ (and, hence, $I_1^{(2)}$) is finite even after removing the ultraviolet regulator, i.e., at
341 $\mu_1 \rightarrow \infty$. It is convenient to introduce the two-body norm $\bar{I}_2^{(2)}$ amputated from the coupling constant squared. By
342 definition, $\bar{I}_2^{(2)} = I_2^{(2)}/g^2$. It does not depend on g . Note that the following identity is valid:

$$\bar{I}_2^{(2)} = -\bar{\Sigma}^{(2)'}(m^2). \quad (54)$$

343 This result can be checked by differentiating the right-hand side of Eq. (48) and comparing the result with the right-
344 hand side of Eq. (53). The derivative $\bar{\Sigma}^{(2)'}(m^2)$ is calculated analytically in Appendix A. Now we obtain for the
345 one-body wave function

$$\psi_1^{(2)} = \sqrt{1 - g^2 \bar{I}_2^{(2)}}. \quad (55)$$

346 Eqs. (51) and (55) determine the normalized (and renormalized) Fock components of the scalar nucleon state vector
347 in the two-body truncation.

348 The two-body wave function is

$$\psi_2^{(2)j}(k_\perp, x) = \frac{\Gamma_2^{(2)}}{s_2^j - m^2} = \frac{gx(1-x)}{k_\perp^2 + \mu_j^2(1-x) + m^2 x^2}. \quad (56)$$

349 In contrast to the vertex function, it depends on both kinematical variables and on the index j .

350

B. Renormalization Parameters

351 To fix all the renormalization parameters, one should relate the bare coupling constant g_{02} with the physical one.
352 Once the Fock components are available, the relation desired can be obtained from Eq. (47):

$$g_{02} = \frac{g}{\psi_1^{(2)}} = \frac{g}{\sqrt{1 - g^2 \bar{I}_2^{(2)}}}. \quad (57)$$

353 Substituting Eq. (57) into Eq. (49), we find the mass counterterm:

$$\delta m_2^2 = \frac{g^2 \bar{\Sigma}^{(2)}(m^2)}{1 - g^2 \bar{I}_2^{(2)}}. \quad (58)$$

354 Then, the field strength renormalization factor defined by Eq. (31),

$$Z_\chi^{(2)} = \left[1 - g_{02}^2 \bar{\Sigma}^{(2)'}(m^2) \right]^{-1} = 1 + g^2 \bar{\Sigma}^{(2)'}(m^2) = 1 - I_2^{(2)} = I_1^{(2)}, \quad (59)$$

355 as expected. In the limit of infinite PV scalar pion mass μ_1 the quantities g_{02} and $Z_\chi^{(2)}$ tend to finite values, while δm_2^2
356 diverges logarithmically, like the self-energy $\bar{\Sigma}^{(2)}$. The bare parameters g_{02} and δm_2^2 defined by Eqs. (57) and (58),
357 respectively, will be used as an input in the next order ($N = 3$) approximation.

358

C. Critical coupling associated with the Landau pole

359 From Eq. (57) it is seen that g_{02}^2 considered as a function of g^2 becomes singular at $g^2 = 1/\bar{I}_2^{(2)}$. A similar singularity
360 arises in the bare coupling of QED and is called the Landau pole³. The critical coupling constant $\alpha = \alpha_L$ associated
361 with the Landau pole is determined by

$$\alpha_L^{-1} = 16\pi m^2 \bar{I}_2^{(2)} = \frac{1}{\pi} \int_0^1 dx \left[\frac{x(1-x)}{(1-x)\mu^2/m^2 + x^2} - \frac{x(1-x)}{(1-x)\mu_1^2/m^2 + x^2} \right], \quad (60)$$

362 where α relates to g by Eq. (4). If $\alpha > \alpha_L$, the bare coupling constant g_{02} becomes imaginary. In principle, one can
363 always adjust the PV scalar pion mass μ_1 to make α_L large enough for the mathematical self-consistency of the model.
364 From physical considerations however it is evident that one has to take $\mu_1 \gg m$ to claim that the renormalization
365 procedure allows one to eliminate the regularization parameters. In the limit $\mu_1 \rightarrow \infty$ Eq. (60) reduces to

$$\alpha_L = \pi \left[\frac{\xi(3 - \xi^2)}{\sqrt{4 - \xi^2}} \arctan \left(\frac{\sqrt{4 - \xi^2}}{\xi} \right) - 1 + (1 - \xi^2) \log \frac{1}{\xi} \right]^{-1}, \quad (61)$$

366 where $\xi = \mu/m$. For $\mu/m = 0.14/0.94$, $\alpha_L \simeq 2.630$. Above the critical coupling, the scalar Yukawa theory becomes
367 ill-defined. At the same time, the threshold of the coupling constant may not be apparent in calculated observables
368 within the two-body truncation, which are well-defined for arbitrary strong coupling. The critical coupling (61)
369 however brings real restrictions on admitted values of α in the three-body truncation, where the renormalized Fock
370 components do not exist at $\alpha > \alpha_L$. We will discuss these points in more detail below.

371

VI. SCALAR NUCLEON STATE VECTOR IN THE THREE-BODY ($N = 3$) TRUNCATION

372

A. Equations for the Fock components and their solution

373 The system of equations for the vertex functions in the three-body Fock space truncation ($N = 3$) is graphically
374 shown in Fig. 6. It differs from that in the $N = 2$ case by the presence of three-body intermediate states which
375 complicate the equations to some extent. According to the FSDR rules [6], the elementary interaction vertices inside
376 full three-body states, (i.e., the vertices appearing simultaneously with a scalar pion spectator), contain the bare
377 coupling constant g_{02} or the mass counterterm δm_2^2 . The interaction vertices with no pion spectator above them
378 correspond to the factors g_{03} or δm_3^2 . The appearance, in different intermediate states, of the sector dependent bare
379 coupling constants, either g_{02} or g_{03} , and the mass counterterms, either δm_2^2 or δm_3^2 , is the very essence of the sector
380 dependent renormalization scheme.

³ In QED, due to the Ward Identity, the renormalization of the charge entirely comes from the vacuum polarization. Our case is different: we exclude the vacuum polarization and, because of the Fock space truncation, the coupling constant renormalization is fully caused by the self-energy correction.

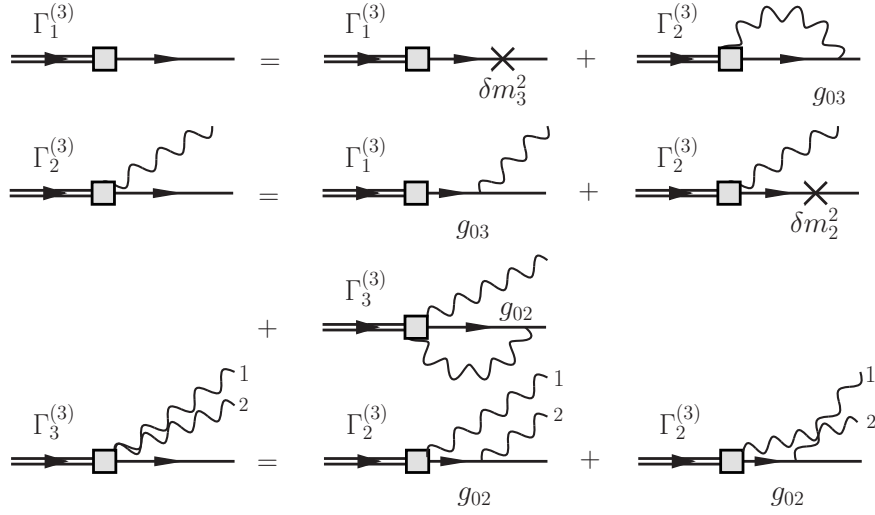


FIG. 6. System of equations for the Fock components in the three-body truncation.

381 When we solve the problem in the three-body truncation, the values g_{02} and δm_2^2 are assumed to be known — they
 382 were obtained in the two-body truncation [see Eqs. (57) and (58)]. The new renormalization parameters g_{03} and δm_3^2
 383 will be found by applying the renormalization conditions again. So, in the framework of FSDR, the refinement of
 384 these quantities from sector to sector is analogous to their refinement, from order to order, in perturbation theory.
 385 As explained in Sec. IV, we need the sector dependent renormalization scheme in order to eliminate divergences for
 386 any given truncation.

Applying the rules of the LFD graph techniques, we cast the system of equations for the vertex functions in the three-body truncation in an analytical form:

$$\Gamma_1^{(3)} = \frac{\delta m_3^2 \Gamma_1^{(3)}}{m^2 - M^2} + g_{03} \sum_{j=0}^1 (-1)^j \int_0^1 \frac{dx}{2x(1-x)} \int \frac{d^2 k_\perp}{(2\pi)^3} \frac{\Gamma_2^{(3)j}(k_\perp, x)}{s_2^j - M^2}, \quad (62)$$

$$\begin{aligned} \Gamma_2^{(3)j}(k_\perp, x) &= \frac{g_{03} \Gamma_1^{(2)}}{m^2 - M^2} + \frac{\delta m_2^2 \Gamma_2^{(3)j}(k_\perp, x)}{(1-x)(s_2^j - M^2)} \\ &+ g_{02} \sum_{j'=0}^1 (-1)^{j'} \int_0^{1-x} \frac{dx'}{2x'(1-x-x')} \int \frac{d^2 k'_\perp}{(2\pi)^3} \frac{\Gamma_3^{(3)jj'}(k_\perp, x, k'_\perp, x')}{s_3^{jj'} - M^2}, \end{aligned} \quad (63)$$

$$\Gamma_3^{(3)jj'}(k_\perp, x, k'_\perp, x') = \frac{g_{02} \Gamma_2^{(3)j}(k_\perp, x)}{(1-x)(s_2^j - M^2)} + \frac{g_{02} \Gamma_2^{(3)j'}(k'_\perp, x')}{(1-x')(s_2^{j'} - M^2)}, \quad (64)$$

387 where s_2^j is defined by Eq. (45), $s_2^{j'}$ is given by the same formula, changing $k_\perp \rightarrow k'_\perp$, $x \rightarrow x'$, and $j \rightarrow j'$, and

$$s_3^{jj'} = \frac{k_\perp^2 + \mu_j^2}{x} + \frac{k'^2_\perp + \mu_{j'}^2}{x'} + \frac{(\mathbf{k}_\perp + \mathbf{k}'_\perp)^2 + m^2}{1-x-x'} \quad (65)$$

388 is the three-body invariant mass squared.

As before, the mass eigenvalue M is implied to be identical to the physical nucleon mass m , i.e., the limit $M \rightarrow m$ should be taken in Eqs. (62)–(64). The three-body vertex function $\Gamma_3^{(3)}$ is expressed through the two-body vertex. Therefore, it can be excluded by substituting Eq. (64) into Eq. (63). The corresponding analytical expression reads

$$\begin{aligned} \left[1 - \frac{g_{02}^2 \bar{\Sigma}^{(2)}(\ell^2) - \delta m_2^2}{\ell^2 - m^2} \right] \Gamma_2^{(3)j}(k_\perp, x) &= g_{03} \psi_1^{(3)} + g_{02}^2 \sum_{j'=0}^1 (-1)^{j'} \int_0^{1-x} \frac{dx'}{2x'(1-x')(1-x-x')} \int \frac{d^2 k'_\perp}{(2\pi)^3} \\ &\times \frac{\Gamma_2^{(3)j'}(k'_\perp, x')}{(s_2^{j'} - m^2)(s_3^{jj'} - m^2)}. \end{aligned} \quad (66)$$

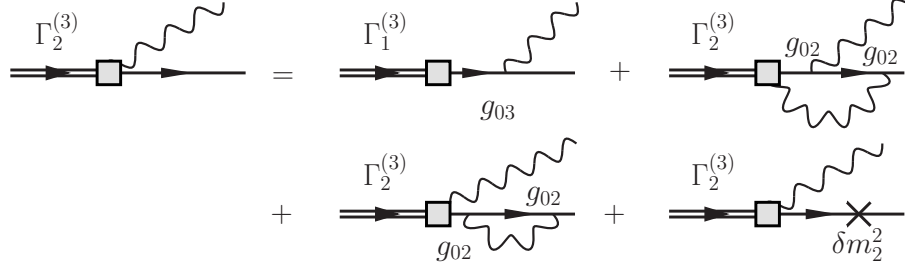


FIG. 7. Equation for the two-body component after the exclusion of the three-body component.

where $\ell^2 = m^2 - (1-x)(s_2^j - m^2)$. The term proportional to the self-energy $\bar{\Sigma}^{(2)}(\ell^2)$ is generated by the substitution of the first addendum on the right-hand side of Eq. (64) into the integral term of Eq. (63). Indeed, the result of this substitution has the form

$$\frac{g_{02}^2 \Gamma_2^{(3)j}(k_\perp, x)}{(1-x)(s_2^j - m^2)} \sum_{j'=0}^1 (-1)^{j'} \int_0^{1-x} \frac{dx'}{2x'(1-x-x')} \int \frac{d^2 k'_\perp}{(2\pi)^3} \frac{1}{s_3^{jj'} - m^2}. \quad (67)$$

Making the sequential change of the integration variables $x' \rightarrow (1-x)x'$ and then $\mathbf{k}'_\perp \rightarrow \mathbf{k}'_\perp - x'\mathbf{k}_\perp$, we can cast the expression (67) in the form

$$\frac{g_{02}^2 \Gamma_2^{(3)j}(k_\perp, x)}{(1-x)(s_2^j - m^2)} \sum_{j'=0}^1 (-1)^{j'} \int_0^1 \frac{dx'}{2x'(1-x')} \int \frac{d^2 k'_\perp}{(2\pi)^3} \frac{1}{s'^{jj'} - \ell^2} = \frac{g_{02}^2 \Gamma_2^{(3)j}(k_\perp, x) \bar{\Sigma}^{(2)}(\ell^2)}{\ell^2 - m^2}, \quad (68)$$

as follows from Eq. (48) and the definition of the quantity ℓ^2 . The latter is nothing else than the square of the off-shell four-momentum of the constituent scalar nucleon in the two-body state: $\ell^2 = (p - k_2)^2$, where k_2 is the scalar pion spectator four-momentum. Note that both the self-energy $g_{02}^2 \bar{\Sigma}^{(2)}(\ell^2)$ and the mass counterterm δm_2^2 diverge logarithmically at large mass μ_1 of the PV scalar pion, but their combination

$$g_{02}^2 \bar{\Sigma}^{(2)}(\ell^2) - \delta m_2^2 = g_{02}^2 \left[\bar{\Sigma}^{(2)}(\ell^2) - \bar{\Sigma}^{(2)}(m^2) \right] \quad (69)$$

entering into Eq. (66) is finite in this limit, provided ℓ^2 is of order of physical masses squared. This cancellation of divergent terms is just an important feature of FSDR. The equation (66) determining the two-body vertex function $\Gamma_2^{(3)j}(k_\perp, x)$ in the three-body truncation is a three-body counterpart of Eq. (47). When $k_\perp \rightarrow \infty$, it turns into $\Gamma_2^{(3)j} \rightarrow g_{03} \psi_1^{(3)}$, which differs from $\Gamma_2^{(2)j}$ by the replacement of the index pointing out the order of truncation.

The substitution of Eq. (64) into Eq. (63), which has been done analytically, could be realized diagrammatically as well. In such a way, we would obtain the graphical equation for the two-body vertex function, shown in Fig. 7. Using the LFD graph techniques rules leads to the same analytical equation (66).

Now we make use of Eqs. (57), (54), and (58) in order to get rid of the second order bare parameters g_{02} and δm_2^2 in Eq. (66). After simple transformations, we arrive at the following equation

$$\left[1 - \frac{g^2 \bar{\Sigma}_r^{(2)}(\ell^2)}{\ell^2 - m^2} \right] \Gamma_2^{(3)j}(k_\perp, x) = g_{03} \psi_1^{(3)} \left[1 - g^2 \bar{I}_2^{(2)} \right] + \frac{g^2}{8\pi^2} \sum_{j'=0}^1 (-1)^{j'} \int_0^{1-x} dx' \int_0^\infty dk'_\perp k'_\perp V^{jj'}(k_\perp, x, k'_\perp, x') \Gamma_2^{(3)j'}(k'_\perp, x'), \quad (70)$$

where

$$\bar{\Sigma}_r^{(2)}(\ell^2) = \bar{\Sigma}^{(2)}(\ell^2) - \bar{\Sigma}^{(2)}(m^2) - \bar{\Sigma}^{(2)'}(m^2)(\ell^2 - m^2) \quad (71)$$

409 is the renormalized scalar nucleon self-energy in the two-body truncation, its argument

$$\ell^2 = -\frac{k_\perp^2}{x} + (1-x)m^2 - \mu_j^2 \left(\frac{1-x}{x} \right), \quad (72)$$

410 and

$$\begin{aligned} V^{jj'}(k_\perp, x, k'_\perp, x') &= \frac{1}{2\pi x'(1-x')(1-x-x')(s_2^{jj'} - m^2)} \int_0^{2\pi} \frac{d\phi'}{s_3^{jj'} - m^2} \\ &= \frac{1}{k_\perp'^2 + \mu_{j'}^2(1-x') + m^2 x'^2} \\ &\quad \times \left[(1-x-x')^2 \left(\frac{k_\perp^2 + \mu_j^2}{x} + \frac{k_\perp'^2 + \mu_{j'}^2}{x'} + \frac{k_\perp^2 + k_\perp'^2 + m^2}{1-x-x'} - m^2 \right)^2 - 4k_\perp^2 k_\perp'^2 \right]^{-1/2}. \end{aligned} \quad (73)$$

411 The integration over the azimuthal angle ϕ' has been done analytically by using the formula

$$\int_0^{2\pi} \frac{d\phi'}{A + B \cos \phi'} = \frac{2\pi}{\sqrt{A^2 - B^2}}, \quad (A^2 > B^2). \quad (74)$$

412 Eq. (70) contains the undefined bare coupling constant g_{03} . To fix it, one should apply the renormalization condi-
413 tion (42) which now becomes

$$\Gamma_2^{(3)j=0}(k_\perp^*(x), x) = g\sqrt{I_1^{(2)}} = g\sqrt{1 - g^2 \bar{I}_2^{(2)}} \quad (75)$$

with $k_\perp^*(x)$ given by Eq. (35). We thus set $k_\perp = k_\perp^*(x)$ and $j = 0$ on both sides of Eq. (70) and demand the condition (75) to hold for arbitrary $0 \leq x \leq 1$. The argument of the self-energy ℓ^2 turns into m^2 at the renormalization point. Taking into account that

$$\bar{\Sigma}_r^{(2)}(\ell^2) \stackrel{\ell^2 \rightarrow m^2}{\sim} (\ell^2 - m^2)^2,$$

414 we get

$$\begin{aligned} g_{03}\psi_1^{(3)} &= \left[1 - g^2 \bar{I}_2^{(2)} \right]^{-1} \\ &\quad \times \left[g\sqrt{1 - g^2 \bar{I}_2^{(2)}} - \frac{g^2}{8\pi^2} \sum_{j'=0}^1 (-1)^{j'} \int_0^{1-x} dx' \int_0^\infty dk'_\perp k'_\perp V^{0j'}(k_\perp^*(x), x, k'_\perp, x') \Gamma_2^{(3)j'}(k'_\perp, x') \right]. \end{aligned} \quad (76)$$

415 An immediate observation is that the right-hand side of Eq. (76) depends on the longitudinal momentum fraction of
416 the scalar pion x . Therefore, we allow g_{03} to depend on x in order to satisfy the condition Eq. (75) for any value of x
417 [7] (see the detailed discussion below, in Sec. VIII). Substituting the combination $g_{03}\psi_1^{(3)}$ back into Eq. (70), we find
418 a closed renormalized equation for the two-body vertex function:

$$\begin{aligned} \left[1 - \frac{g^2 \bar{\Sigma}_r^{(2)}(\ell^2)}{\ell^2 - m^2} \right] \Gamma_2^{(3)j}(k_\perp, x) &= g\sqrt{1 - g^2 \bar{I}_2^{(2)}} \\ &\quad + \frac{g^2}{8\pi^2} \sum_{j'=0}^1 (-1)^{j'} \int_0^{1-x} dx' \int_0^\infty dk'_\perp k'_\perp \Delta V^{jj'}(k_\perp, x, k'_\perp, x') \Gamma_2^{(3)j'}(k'_\perp, x'), \end{aligned} \quad (77)$$

419 where

$$\Delta V^{jj'}(k_\perp, x, k'_\perp, x') = V^{jj'}(k_\perp, x, k'_\perp, x') - V^{0j'}(k_\perp^*(x), x, k'_\perp, x'). \quad (78)$$

420 In fact, Eq. (77) is a system of two inhomogeneous linear integral equations for the two components of $\Gamma_2^{(3)j}$ (i.e., those
 421 with $j = 0$ and $j = 1$). These equations are fully nonperturbative. On solving them, we obtain a properly normalized
 422 two-body vertex function $\Gamma_2^{(3)j}(k_\perp, x)$. Eq. (64) taken for $M = m$ uniquely determines the three-body vertex function
 423 $\Gamma_3^{(3)jj'}(k_\perp, x, k'_\perp, x')$ in terms of the two-body vertex function. The one-body wave function $\psi_1^{(3)}$ is then found from
 424 the normalization condition for the whole state vector:

$$\psi_1^{(3)} = \sqrt{I_1^{(3)}} = \sqrt{1 - I_2^{(3)} - I_3^{(3)}}, \quad (79)$$

425 where the two- and three-body Fock sector norms are calculated according to Eq. (40) with $N = 3$, taking into account
 426 PV particle contributions:

$$I_2^{(3)} = \int_0^1 \frac{dx}{2x(1-x)} \int \frac{d^2 k_\perp}{(2\pi)^3} \sum_{j=0}^1 (-1)^j \left[\frac{\Gamma_2^{(3)j}(k_\perp, x)}{s_2^j - m^2} \right]^2, \quad (80)$$

$$I_3^{(3)} = \frac{1}{2} \int_0^1 \frac{dx}{2x} \int \frac{d^2 k_\perp}{(2\pi)^3} \int_0^{1-x} \frac{dx'}{2x'(1-x-x')} \int \frac{d^2 k'_\perp}{(2\pi)^3} \sum_{j,j'=0}^1 (-1)^{j+j'} \left[\frac{\Gamma_3^{(3)jj'}(k_\perp, x, k'_\perp, x')}{s_3^{jj'} - m^2} \right]^2. \quad (81)$$

427 We emphasize that all Fock components of the scalar nucleon state vector in the three-body truncation can be
 428 calculated without any reference to Eq. (62) which determines the mass counterterm δm_3^2 . Together with the bare
 429 coupling constant g_{03} , it will be needed in higher order ($N \geq 4$) truncations only. This feature reflects a general
 430 property of FSDR: the highest order bare parameters g_{0N} and δm_N^2 found in the N -body truncation are actually
 431 needed, starting from the $(N + 1)$ -body truncation.

432 If we restrict our consideration of the scalar Yukawa model to calculations of observables inside the three-body
 433 approximation, we may completely get rid of PV particles, assuming the limit $\mu_1 \rightarrow \infty$. Once logarithmic divergences
 434 coming from the self-energy and the mass counterterm are mutually canceled in their combination (69), one can
 435 take the limit $\mu_1 \rightarrow \infty$ directly in Eq. (77) by omitting all contributions with either $j = 1$ or $j' = 1$. The reason
 436 is that the kernel V^{00} , Eq. (73) at $j = j' = 0$, does not produce new divergences requiring regularization by PV
 437 particles. This does not mean that we would automatically get $\Gamma_2^{(3)j=1} = 0$ in the limit $\mu_1 \rightarrow \infty$. The PV components
 438 of the vertex functions may tend to a finite nonzero limit, but they do not affect the physical components or the
 439 calculated observables, or the Fock sector norms (79)–(81). This statement relates to both the two- and three-body
 440 vertices and reasonably simplifies subsequent numerical calculations. Note that in the spinor Yukawa model, where
 441 divergences are stronger, such a procedure does not work and one has to retain PV particle contributions till the end
 442 of calculations [7, 16].

443 The inhomogeneous linear integral equation (77) was solved numerically for various values of the physical coupling
 444 constant α defined by Eq. (4) and the physical particle masses $m = 0.94$ and $\mu = 0.14$. To find the solution we
 445 employ an iterative method. We first approximate the integrals by using Gauss-Legendre quadratures. We start with
 446 an educated guess for $\Gamma_2^{(3)j}$ and substitute it onto the right-hand side of Eq. (77). We solve for $\Gamma_2^{(3)j}$ on the left-hand
 447 side on the quadrature grid, interpolating as needed. The obtained $\Gamma_2^{(3)j}$ then serves as the input for the next round
 448 of iterations. We update $\Gamma_2^{(3)j}$ until the point-by-point total deviation is sufficiently small.

449 Representative solutions for $\Gamma_2^{(3)j=0}(k_\perp, x)$ are shown in Fig. 8. We removed the PV mass by taking the limit
 450 $\mu_1 \rightarrow \infty$.⁴ The curves in Fig. 8 reflect typical behavior of $\Gamma_2^{(3)j=0}(k_\perp, x)$ as a function of its arguments.

452 Our calculations distinctly indicate that the physical coupling constant α cannot be taken arbitrarily large. If we
 453 fix x and consider $\Gamma_2^{(3)j=0}$ as a function of k_\perp , its limiting ($k_\perp \rightarrow \infty$) value rapidly increases in magnitude with the
 454 increase of α . The same happens in the limit $x \rightarrow 0$ at fixed k_\perp . At certain $\alpha = \alpha_c$ it seems that $\Gamma_2^{(3)j=0}$ becomes
 455 unbounded. Further increase of α leads to the absence of stable numerical solutions of Eq. (77). Numerical estimations
 456 give $\alpha_c \simeq 2.630$. In the next section we will explain the reason why the critical coupling appears in the given physical
 457 model and calculate α_c exactly.

⁴ The limiting solution for $\Gamma_2^{(3)j=0}$ is sufficient for calculations within the three-body Fock space truncation, but the solution with a finite PV mass is useful in the four-body truncation, where the PV mass cannot be easily removed.

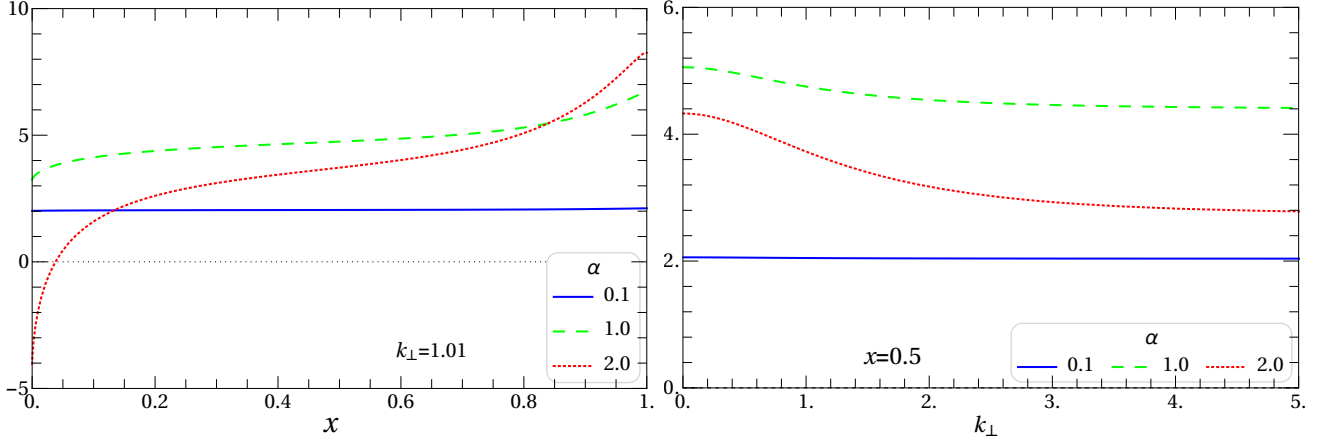


FIG. 8. The vertex function $\Gamma_2^{(3)j=0}(k_\perp, x)$ as a function of x at fixed k_\perp (left panel), and as a function of k_\perp at fixed x (right panel), calculated in the three-body truncation for several values of the physical coupling constant α . The PV mass has been removed by taking the limit $\mu_1 \rightarrow \infty$.

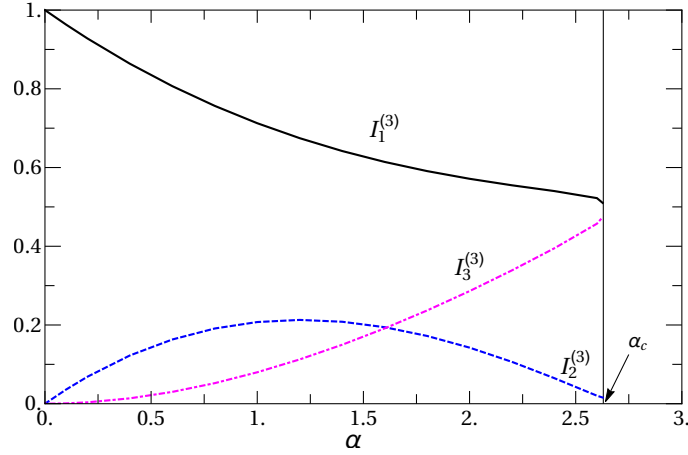


FIG. 9. Fock sector norms in the three-body truncation as a function of the physical coupling constant α .

458 To estimate relative contributions of different Fock sectors to the full state vector norm, we calculated the corre-
 459 sponding sector norms as a function of the coupling constant which varies from zero up to the critical value. The
 460 results are presented in Fig. 9. One observes that the one-body sector always dominates, though its contribution
 461 monotonically decreases with the increase of the coupling constant. The behavior of the two-body sector contribution
 462 looks nontrivial: it increases to a maximum and then decreases as a function of the coupling constant. The three-body
 463 sector contribution increases monotonically, but it does not reach the value of the one-body sector contribution.

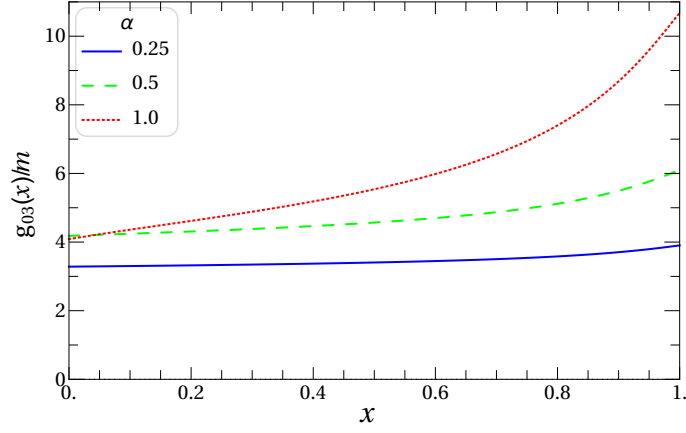


FIG. 10. Ratio $g_{03}(x)/m$ as a function of x for a few values of α .

464

B. Renormalization Parameters

465 Having found $\Gamma_2^{(3)j}(k_\perp, x)$ and $\psi_1^{(3)}$, we can calculate the bare coupling constant $g_{03} = g_{03}(x)$ from Eq. (76):

$$\begin{aligned}
 g_{03}(x) = & \frac{1}{\sqrt{I_1^{(3)}}} \left[\frac{g}{\sqrt{1 - g^2 \bar{I}_2^{(2)}}} \right. \\
 & - \frac{g^2}{8\pi^2 [1 - g^2 \bar{I}_2^{(2)}]} \sum_{j'=0}^1 (-1)^{j'} \int_0^{1-x} dx' x' \int_0^\infty \frac{k'_\perp dk'_\perp}{k'^2_\perp + \mu_{j'}^2 (1-x') + m^2 x'^2} \\
 & \left. \times \frac{\Gamma_2^{(3)j'}(k'_\perp, x')}{\sqrt{[k'^2_\perp (1-x) + m^2 x'^2 (1+x) - \mu^2 x'^2 + \mu_{j'}^2 (1-x-x')]^2 + 4k'^2_\perp [m^2 x'^2 + \mu^2 (1-x)] x'^2}} \right]. \quad (82)
 \end{aligned}$$

466 Note that the integrand in Eq. (82) is not singular even without PV regularization and the term with $j' = 1$ in the sum
 467 vanishes in the limit $\mu_1 \rightarrow \infty$. Therefore, $g_{03}(x)$ does not contain divergences. As outlined above, it does explicitly
 468 depend on x .

469 In Fig. 10 we show the dependence of g_{03} , in units m , on the kinematical variable x for several values of the
 470 physical coupling constant α . If rotational symmetry was not broken by the Fock space truncation, g_{03} would be a
 471 true constant independent of x . As is seen from Fig. 10, this is not the case: g_{03} depends on x ; the larger the value
 472 of α the stronger is the x -dependence. Such a property is a price we pay to have the renormalization condition (75)
 473 satisfied for arbitrary x . The question of x -dependence of g_{03} is discussed below in a special Sec. VIII.

474 Similarly, the three-body mass counterterm δm_3^2 can be found from Eq. (62) in the limit $M \rightarrow m$, taking into
 475 account the x -dependence of g_{03} :

$$\delta m_3^2 = - \frac{1}{8\pi^2 \sqrt{I_1^{(3)}}} \sum_{j=0}^1 (-1)^j \int_0^1 dx g_{03}(x) \int_0^\infty dk_\perp k_\perp \frac{\Gamma_2^{(3)j}(k_\perp, x)}{k_\perp^2 + \mu_j^2 (1-x) + m^2 x^2}. \quad (83)$$

476 In contrast to $g_{03}(x)$, the mass counterterm δm_3^2 is a true constant independent of kinematical variables. If $\mu_1 \rightarrow \infty$,
 477 δm_3^2 diverges like $\log(\mu_1/m)$, i.e., one cannot avoid PV particle contributions, when calculating it.

478 A question may arise, why one should insert $g_{03}(x)$ into the integrand in Eq. (83), rather than to leave it as a
 479 free factor [like it appears originally in Eq. (62)], making δm_3^2 to be x -dependent as well. An answer can not be
 480 found in the framework of the three-body Fock space truncation, and the above recipe appears as an ansatz. The
 481 rule is however justified in the four-body truncation [8, 9], where $g_{03}(x)$ and δm_3^2 are necessary to calculate the Fock

482 components. It can be easily seen that $g_{03}(x)$ enters into amplitudes of light-front diagrams constructed according to
483 the FSDR requirements, being integrated over dx .

484 It is instructive to consider not only the mass counterterm δm_3^2 , but also the three-body self-energy [cf. Eq. (48)]:

$$\Sigma^{(3)}(p^2) = -\frac{1}{\sqrt{I_1^{(3)}}} \sum_{j=0}^1 (-1)^j \int_0^1 \frac{dx g_{03}(x)}{2x(1-x)} \int \frac{d^2 k_\perp}{(2\pi)^3} \frac{\Gamma_2^{(3)j}(k_\perp, x; p^2)}{s_2^j - p^2} \quad (84)$$

485 with $\delta m_3^2 = \Sigma^{(3)}(m^2)$. $\Gamma_2^{(3)j}(k_\perp, x; p^2)$ is the fully off-energy-shell two-body vertex function, i.e., that introduced in
486 Eq. (28) with $M^2 = p^2 \neq m^2$. It satisfies the same integral equation (63), changing M^2 to p^2 , with the renormalization
487 condition $\Gamma_2^{(3)j=0}(k_\perp^*(x), x; m^2) = g\sqrt{I_1^{(3)}}$. After simple transformations, fully analogous to those made above, one
488 can derive the following renormalized equation for it:

$$\begin{aligned} \left[1 - \frac{g^2 \bar{\Sigma}_r^{(2)}(\ell_p^2)}{\ell_p^2 - m^2} \right] \Gamma_2^{(3)j}(k_\perp, x; p^2) &= g \sqrt{1 - g^2 \bar{I}_2^{(2)}} \\ &+ \frac{g^2}{8\pi^2} \sum_{j'=0}^1 (-1)^{j'} \int_0^{1-x} dx' \int_0^\infty dk'_\perp k'_\perp \\ &\times \left[V^{jj'}(k_\perp, x, k'_\perp, x'; p^2) \Gamma_2^{(3)j'}(k'_\perp, x'; p^2) \right. \\ &\left. - V^{0j'}(k_\perp^*(x), x, k'_\perp, x'; m^2) \Gamma_2^{(3)j'}(k'_\perp, x'; m^2) \right], \end{aligned} \quad (85)$$

489 where $\ell_p^2 = -\frac{k_\perp^2}{x} + p^2(1-x) - \mu_j^2 \left(\frac{1-x}{x}\right)$ and

$$\begin{aligned} V^{jj'}(k_\perp, x, k'_\perp, x'; p^2) &= \frac{1}{k_\perp'^2 + \mu_{j'}^2(1-x') + m^2 x' - p^2 x'(1-x')} \\ &\times \left[(1-x-x')^2 \left(\frac{k_\perp^2 + \mu_j^2}{x} + \frac{k_\perp'^2 + \mu_{j'}^2}{x'} + \frac{k_\perp^2 + k_\perp'^2 + m^2}{1-x-x'} - p^2 \right)^2 - 4k_\perp^2 k_\perp'^2 \right]^{-1/2}. \end{aligned} \quad (86)$$

490 The derivative $\Sigma^{(3)'}(m^2)$ is related to the field strength renormalization factor

$$Z_\chi^{(3)} = \left[1 - \Sigma^{(3)'}(m^2) \right]^{-1}. \quad (87)$$

491 In spite of both $\Sigma^{(3)}(p^2)$ and $\Gamma_2^{(3)j}(k_\perp, x; p^2)$ having a three-body “origin”, they are actually not needed within the
492 three-body truncation, like δm_3^2 and g_{03} . So, without going beyond the $N = 3$ case, one may ignore the properties of
493 these off-shell quantities. The latter quantities however naturally appear, when finding the Fock components in the
494 four-body truncation, where they affect the calculated results in full measure. In particular, the fully off-energy-shell
495 two-body vertex function $\Gamma_2^{(3)j}(k_\perp, x; p^2)$ is a source of the critical value of the coupling constant for $N = 4$. This
496 point is discussed in more detail in the next section.

498 The comparison of the calculated value of the field strength renormalization factor $Z_\chi^{(3)}$ with the one-body normal-
499 ization integral $I_1^{(3)}$ serves as an additional test of our numerical computations. As is seen from Fig. 11, these two
500 quantities do coincide with each other within the numerical precision.

501

C. Critical coupling

502 The parameters entering into the linear integral equation (77) — the coupling constant g and the particle masses
503 — should be chosen to allow a physically proper solution for the two-body vertex function. We will not perform here

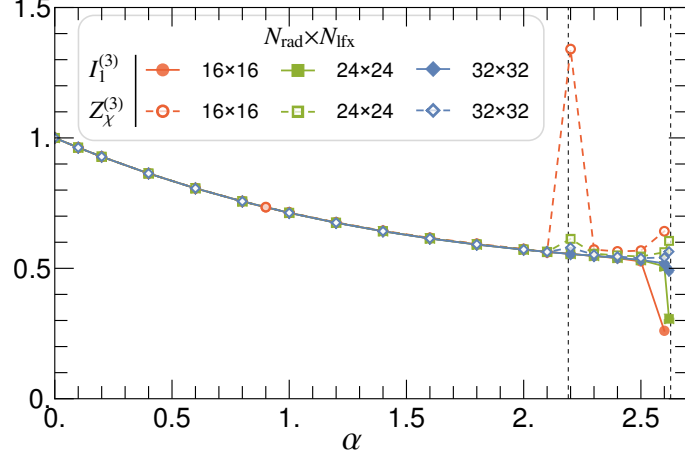


FIG. 11. Comparison of the one-body norm $I_1^{(3)}$ and the field strength renormalization factor $Z_\chi^{(3)}$. N_{rad} and N_{fix} are, respectively, the numbers of Gaussian integration nodes in the variables k_\perp and x . $I_1^{(3)}$ is obtained from the wave function normalization, Eq. (79). $Z_\chi^{(3)}$ is obtained from the self-energy (84) by means of Eq. (87). These two quantities agree within the numerical precision. The dashed lines mark the positions of the critical coupling constants $\alpha_c^{\text{nr}} \simeq 2.190$ (see Sec. VIC below) and $\alpha_c \simeq 2.630$.

504 the full analysis, but study the behavior of $\Gamma_2^{(3)j}$ as a function of g for fixed values of the particle masses m and μ .
 505 Some of our conclusions can be proven analytically, while we will rely on the results of numerical computations for
 506 the remainder.

507 For simplicity, we consider the case of an infinite PV mass μ_1 . As discussed above, this limit is reached by omitting
 508 the term with $j' = 1$ in the sum in Eq. (77). We thus obtain a single linear integral equation for $\Gamma_2^{(3)j=0}(k_\perp, x)$ which
 509 we will denote here simply Γ_2 , for brevity. Then we represent Eq. (77) in the following operator form:

$$\Gamma_2 = f + \hat{\mathbf{A}}\Gamma_2, \quad (88)$$

510 where $f = g\sqrt{1 - g^2\bar{I}_2^{(2)}}$ is the inhomogeneous part, and the operator $\hat{\mathbf{A}}$ is represented as a sum of the two contributions

$$\hat{\mathbf{A}} = \hat{\mathbf{A}}' + \hat{\mathbf{K}}, \quad (89)$$

511 where

$$\hat{\mathbf{A}}'\Gamma_2 = \mathcal{F}(\ell^2)\Gamma_2^{(3)j=0}(k_\perp, x), \quad (90)$$

$$\hat{\mathbf{K}}\Gamma_2 = \frac{g^2}{8\pi^2} \int_0^{1-x} dx' \int_0^\infty dk'_\perp k'_\perp \Delta V^{00}(k_\perp, x, k'_\perp, x')\Gamma_2^{(3)j=0}(k'_\perp, x'), \quad (91)$$

512 collect, respectively, all nonintegral and integral terms coming from the interaction in the three-body states. The
 513 function

$$\mathcal{F}(\ell^2) \equiv \frac{g^2\bar{\Sigma}_r^{(2)}(\ell^2)}{\ell^2 - m^2}, \quad (92)$$

514 where ℓ^2 is given by Eq. (72) with $j = 0$, is generated by the scalar nucleon self-energy. The formal solution of
 515 Eq. (88), which can be written as $\Gamma_2 = (1 - \hat{\mathbf{A}})^{-1}f$, is regular, if the operator $(1 - \hat{\mathbf{A}})$ is nonsingular. To find out
 516 conditions when this is satisfied, we consider a more general eigenvalue problem for the operator $\hat{\mathbf{A}}$:

$$\lambda\Gamma_2 = \hat{\mathbf{A}}\Gamma_2. \quad (93)$$

517 Varying the physical coupling constant, we can trace the behavior of the eigenvalues λ . As soon as we encounter at
 518 least one eigenvalue $\lambda = 1$, the solution of Eq. (88) becomes singular.

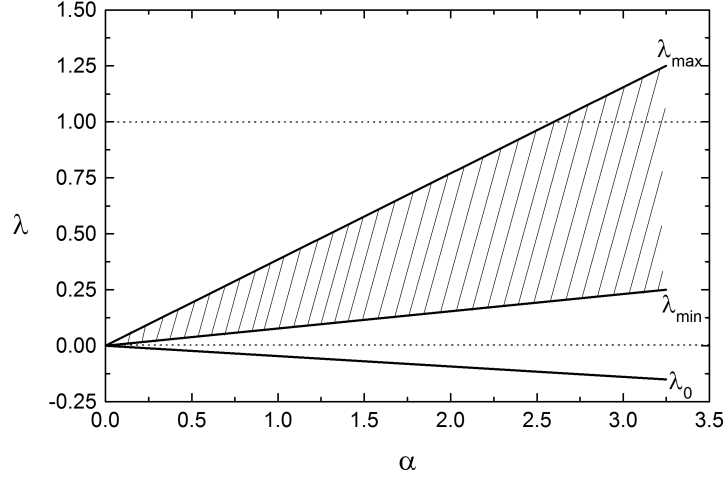


FIG. 12. Eigenvalue spectrum of Eq. (93) as a function of the physical coupling constant α . The cross-hatched region represents the continuous part of the spectrum, while λ_0 is a discrete eigenvalue.

519 For numerical analysis, we represent the operator \hat{A} in a matrix form. It can be achieved by discretizing the integrals
 520 in Eq. (91) by means of the Gaussian procedure. The same is done for the operator \hat{A}' which is reduced to a diagonal
 521 matrix. We thus approximate the operator \hat{A} by a finite $n_A \times n_A$ matrix with the dimension $n_A = n_k n_x$, where n_k
 522 and n_x are the numbers of the integration nodes in the variables k'_\perp and x' , respectively. After this transformation,
 523 we calculate all the n_A eigenvalues λ . Gradually increasing n_A , we analyze the spectrum each time till the eigenvalues
 524 which are interesting for us become stable.

525 It is more convenient to work with the dimensionless coupling constant α related to g^2 by Eq. (4). Evidently, at
 526 $\alpha = 0$ we have a trivial result $\hat{A} = 0$ and the only eigenvalue is $\lambda = 0$. Once α starts increasing, the eigenvalues are
 527 concentrated in a region of a finite size. We are interested in the maximal real eigenvalue λ_{\max} . Varying α , we get a
 528 function $\lambda_{\max}(\alpha)$. The minimal positive root of the equation $\lambda_{\max}(\alpha) = 1$ just gives the critical coupling constant α_c .

529 The calculated spectrum includes one discrete eigenvalue $\lambda_0(\alpha)$ and a set of $(n_A - 1)$ eigenvalues distributed, almost
 530 uniformly, in the interval

$$\lambda_{\min}(\alpha) < \lambda < \lambda_{\max}(\alpha). \quad (94)$$

531 $\lambda_0(\alpha)$ is always negative and therefore has no relation to the critical coupling. Note that all the three functions
 532 $\lambda_0(\alpha)$, $\lambda_{\min}(\alpha)$, and $\lambda_{\max}(\alpha)$ are very stable as n_A increases, while the density of λ 's between $\lambda_{\min}(\alpha)$ and $\lambda_{\max}(\alpha)$
 533 grows. This provides a hint that the exact spectrum consists of two parts: a discrete one including the only eigenvalue
 534 $\lambda_0(\alpha)$ plus a continuous one given by the interval $[\lambda_{\min}(\alpha), \lambda_{\max}(\alpha)]$. The results of the numerical calculation of the
 535 spectrum for $m = 0.94$ and $\mu = 0.14$ are shown in Fig. 12. Note that the functions $\lambda_0(\alpha)$, $\lambda_{\min}(\alpha)$, and $\lambda_{\max}(\alpha)$ are
 536 linear, because the operator \hat{A} is proportional to α . The relative computational precision is about 10^{-5} , corresponding
 537 to $n_A \sim 10^4$. When α increases, $\lambda_{\max}(\alpha)$ reaches unity at $\alpha = \alpha_c \simeq 2.630$.

539 Our calculation revealed an interesting fact: the continuous part (94) of the spectrum is insensitive to the integral
 540 part (91) of the operator \hat{A} . In other words, if we calculate the eigenvalue spectrum of \hat{A}' by means of the matrix
 541 equation

$$\lambda' \Gamma'_2 = \hat{A}' \Gamma'_2, \quad (95)$$

542 then we see that all n_A eigenvalues are confined into an interval with the same boundaries $\lambda_{\min}(\alpha)$ and $\lambda_{\max}(\alpha)$, in
 543 spite of the fact that the eigenvectors Γ_2 and Γ'_2 are different. The coincidence of the continuous parts of the spectra

544 λ and λ' is not caused by chance but originates from some common property of Eqs. (93) and (95), which will be clear
 545 now. The merit of Eq. (95) consists in that it can be trivially solved analytically. Indeed, because of the diagonal
 546 form of the matrix $\hat{\mathbf{A}}'$ the eigenvalues λ' are simply the values of the function $\mathcal{F}(\ell^2)$ at the node points. If $n_A \rightarrow \infty$,
 547 the spectrum becomes continuous:

$$\lambda_{\min}(\alpha) < \lambda' < \lambda_{\max}(\alpha), \quad (96)$$

548 where

$$\lambda_{\min}(\alpha) = \min_{\ell^2} \mathcal{F}(\ell^2), \quad (97)$$

$$\lambda_{\max}(\alpha) = \max_{\ell^2} \mathcal{F}(\ell^2). \quad (98)$$

549 It is easy to check that for $0 \leq k_{\perp} < \infty$ and $0 \leq x \leq 1$ we have $-\infty < \ell^2 \leq (m - \mu)^2$.

550 The condition (96) has very simple meaning. It means that there always exists such a point (k_{\perp}, x) where the
 551 solution of the inhomogeneous equation

$$\lambda' \Gamma'_2 = f + \hat{\mathbf{A}}' \Gamma'_2, \quad (99)$$

552 which is

$$\Gamma'_2 = \frac{f}{\lambda' - \mathcal{F}(\ell^2)}, \quad (100)$$

553 becomes singular. The corresponding equation with the whole operator $\hat{\mathbf{A}}$, Eq. (89),

$$\lambda \Gamma_2 = f + \hat{\mathbf{A}} \Gamma_2, \quad (101)$$

554 which is a generalization of our initial equation (88), can not be solved in a similar trivial way, but its formal “solution”
 555 can be written

$$\Gamma_2 = \frac{f + \hat{\mathbf{K}} \Gamma_2}{\lambda - \mathcal{F}(\ell^2)}. \quad (102)$$

556 Both expressions on the right-hand sides of Eqs. (100) and (102) have denominators of the same type. Assume we
 557 take some value λ inside the interval (94) with the boundaries defined by Eqs. (97) and (98). Then the equation
 558 $\mathcal{F}(\ell^2) = \lambda$ determines a point ℓ^2 [or a set of points (k_{\perp}, x)] where the denominator in Eq. (102) vanishes. The solution
 559 is singular, unless

$$\hat{\mathbf{K}} \Gamma_2 = -f \quad (103)$$

560 at the same point. As our analysis shows, this condition is not satisfied. Hence, the stability of the solution of Eq. (77)
 561 relates to the function $\mathcal{F}(\ell^2)$ only. The critical coupling constant is derived from the equation

$$\max_{\ell^2} \mathcal{F}(\ell^2) = 1, \quad (104)$$

where $-\infty < \ell^2 \leq (m - \mu)^2$. To find the maximum, we make use of the explicit form of $\mathcal{F}(\ell^2)$:

$$\mathcal{F}(\ell^2) = -g^2 \bar{\Sigma}^{(2)'}(m^2) + g^2 \frac{\bar{\Sigma}^{(2)}(\ell^2) - \bar{\Sigma}^{(2)}(m^2)}{\ell^2 - m^2}.$$

Since $\bar{\Sigma}^{(2)'}(\ell^2) < 0$ [this is distinctly seen, e.g., from Eq. (48)], the difference $\bar{\Sigma}^{(2)}(\ell^2) - \bar{\Sigma}^{(2)}(m^2)$ is always positive, while the difference $\ell^2 - m^2$ is negative. So, the quantity $[\bar{\Sigma}^{(2)}(\ell^2) - \bar{\Sigma}^{(2)}(m^2)]/(\ell^2 - m^2)$ is negative. Its maximal (asymptotic) value equals zero, being achieved at $\ell^2 \rightarrow -\infty$. Hence,

$$\max_{\ell^2} \mathcal{F}(\ell^2) = -g^2 \bar{\Sigma}^{(2)'}(m^2)$$

562 and

$$\alpha_c = - \left[16\pi m^2 \bar{\Sigma}^{(2)'}(m^2) \right]^{-1}. \quad (105)$$

563 Substituting here the explicit form (A8) of the derivative of the self-energy, it is easy to see that α_c is identical to the
 564 critical coupling constant α_L associated with the Landau pole (61). For $m = 0.94$ and $\mu = 0.14$ we obtain $\alpha_c \simeq 2.630$,
 565 in full agreement with the value found numerically.

566 Note that α_L naturally appears within the two-body approximation, where it nevertheless does not impose any
 567 restrictions on the calculated renormalized Fock components. In the three-body case discussed here it appears again
 568 but now it substantially affects the behavior of the Fock components. Indeed, for coupling constants above α_c the
 569 equation (77) has no physically acceptable solutions. An attempt to calculate the vertex functions numerically for
 570 $\alpha > \alpha_c$ fails: the calculated results oscillate strongly, when the number of integration nodes n_A increases, without
 571 any tendency to converge. At $\alpha = \alpha_c$ the solution of Eq. (77) is stable.

572 We emphasize that the result $\alpha_c = \alpha_L$ obtained above should be considered as a feature of the Yukawa model
 573 rather than a fundamental property of FSDR in the given approximation. The value of the critical coupling constant
 574 depends on the particular form of the interaction and can hardly be predicted before analyzing the equations for the
 575 Fock components. Indeed, the full eigenvalue spectrum of the equation (93) is determined by the behavior of the
 576 self-energy $\bar{\Sigma}^{(2)}$ and the kernel ΔV as a function of their arguments. In the Yukawa model, the integral part (91) of the
 577 operator \hat{A} generates the only eigenvalue $\lambda_0(\alpha)$ [in addition to the continuous spectrum governed by the self-energy
 578 contribution (90)] having no influence on the stability of the solution. As a result, α_c is fully determined by the
 579 two-body self-energy, which just makes α_c identical to α_L . For another dynamical model, different from the Yukawa
 580 model, the situation may be different.

581 Going over to a finite PV particle mass does not change the qualitative conclusions, but the numerical value of the
 582 critical coupling constant increases. This is not surprising due the fact that each PV subtraction effectively reduces
 583 the interaction strength. So, the case $\mu_1 \rightarrow \infty$ analyzed above brings the tightest limitations on admissible values of
 584 the coupling constant.

585 We thus establish that the solution of the renormalized equation (77) is nonsingular at $\alpha \leq \alpha_c$. This statement
 586 however does not concern the initial, nonrenormalized, equation (70), if the inhomogeneous part $g_{03}\psi_1^{(3)}[1 - g^2\bar{I}_2^{(2)}]$ is
 587 considered as a free parameter (or an independent function of kinematical variables). Numerical computations show
 588 that its solution becomes singular at a lower value of the coupling constant $\alpha = \alpha_c^{\text{nr}}$, where $\alpha_c^{\text{nr}} < \alpha_c$. The new
 589 critical coupling constant now essentially depends on the kernel V of the integral term in Eq. (70). If we perform the
 590 eigenvalue analysis of Eq. (70) (more precisely, of the corresponding homogeneous equation), we will see the following.
 591 The self-energy contribution which is the same as in the renormalized equation (77) generates the continuous part of
 592 the eigenvalue spectrum (94), as previously, but the discrete eigenvalue $\lambda_0(\alpha)$ now is different from that found for the
 593 renormalized equation. Moreover, it is positive and always exceeds the upper boundary of the continuous spectrum
 594 $\lambda_{\text{max}}(\alpha)$, in contrast to the situation shown in Fig. 12. The critical coupling constant α_c^{nr} is found as a root of the
 595 equation $\lambda_0(\alpha_c^{\text{nr}}) = 1$. Numerical calculations performed for $m = 0.94$, $\mu = 0.14$, and an infinite PV mass μ_1 give
 596 $\alpha_c^{\text{nr}} \simeq 2.190$. One may conclude that the renormalization removes the singularity of the solution for the two-body
 597 vertex function, which appears in the original nonrenormalized equation at $\alpha = \alpha_c^{\text{nr}}$.

598 Considering the renormalized equation (85) for the fully off-energy-shell two-body vertex $\Gamma_2^{(3)j}(k_\perp, x; p^2)$, we en-
 599 counter a critical coupling constant $\alpha = \alpha_c^{\text{off}}(p^2)$, depending on p^2 , which makes $\Gamma_2^{(3)j}(k_\perp, x; p^2)$ singular. This
 600 singularity exists only if $p^2 \neq m^2$. On the mass shell, when we take $p^2 = m^2$, the singularity of $\Gamma_2^{(3)j}(k_\perp, x; m^2)$ vs. α
 601 is absent. Without discussing all technical details, we briefly explain below the origin of $\alpha_c^{\text{off}}(p^2)$ and reveal its role in
 602 the calculation of Fock components within the FSDR scheme.

603 Eq. (85) can be solved in two steps. First, we pay attention that setting $p^2 = m^2$ returns us to the renormalized
 604 equation (77), because $\Gamma_2^{(3)j}(k_\perp, x; m^2) \equiv \Gamma_2^{(3)j}(k_\perp, x)$. In the second step, on finding the latter function, we can
 605 reduce Eq. (85) to

$$\left[1 - \frac{g^2 \bar{\Sigma}_r^{(2)}(\ell_p^2)}{\ell_p^2 - m^2} \right] \Gamma_2^{(3)j}(k_\perp, x; p^2) = G_0(x) + \frac{g^2}{8\pi^2} \sum_{j'=0}^1 (-1)^{j'} \int_0^{1-x} dx' \\ \times \int_0^\infty dk'_\perp k'_\perp V^{jj'}(k_\perp, x, k'_\perp, x'; p^2) \Gamma_2^{(3)j'}(k'_\perp, x'; p^2), \quad (106)$$

606 where the inhomogeneous part given by

$$G_0(x) = g\sqrt{1 - g^2 I_2^{(2)}} - \frac{g^2}{8\pi^2} \sum_{j'=0}^1 (-1)^{j'} \int_0^{1-x} dx' \int_0^\infty dk'_\perp k'_\perp V^{0j'}(k'_\perp(x), x, k'_\perp, x'; m^2) \Gamma_2^{(3)j'}(k'_\perp, x'; m^2) \quad (107)$$

607 is already known. As advocated above, the function $\Gamma_2^{(3)j}(k_\perp, x; m^2)$ is nonsingular at $\alpha \leq \alpha_c$. Under this condition,
 608 the function $G_0(x)$ is also a finite quantity. Eq. (106) now has the same shape as the nonrenormalized equation (70)
 609 for the half-off-shell two-body vertex function $\Gamma_2^{(3)j}(k_\perp, x)$, excepting the fact that the kernel parametrically depends
 610 on p^2 . Applying the same eigenvalue analysis, as for Eq. (70) above, we calculate the critical coupling constants
 611 $\alpha_c^{\text{off}}(p^2)$. Note that

$$\alpha_c^{\text{nr}} = \alpha_c^{\text{off}}(m^2). \quad (108)$$

612 The right-hand side of Eq. (108) should be understood as a limit $\alpha_c^{\text{off}}(p^2 \rightarrow m^2)$, because at $p^2 = m^2$, as has been
 613 mentioned above, the two-body vertex function is smooth, even at $\alpha = \alpha_c^{\text{off}}(m^2)$. Then, since the critical coupling
 614 constant α_c defined by Eq. (105) always exists for any of Eqs. (70), (77), and (85), the coupling constant $\alpha_c^{\text{off}}(p^2)$
 615 brings new information, only if $\alpha_c^{\text{off}}(p^2) < \alpha_c$. We emphasize that if $\alpha \leq \alpha_c$ and $\alpha \neq \alpha_c^{\text{off}}(p^2)$, the solutions of
 616 Eqs. (70), (77), and (85) are nonsingular.

617 The critical coupling constants considered above may generate some peculiarities in α -dependence of numerically
 618 calculated quantities, especially when using rough computational grids. Indeed, while the exact result is nonsingular,
 619 the cancellation of pole contributions may not occur in full measure, due to approximate character of numerical
 620 calculations. For instance, sharp behavior of the field strength renormalization factor $Z_\chi^{(3)}$ in the vicinity of the point
 621 $\alpha = \alpha_c^{\text{nr}} = 2.190$ for a relatively small number of Gaussian integration nodes (see Fig. 11) is a probable manifestation
 622 of this effect.

623 The situation with the simultaneous existence of several types of critical coupling constants looks, at first glance,
 624 rather confusing. In order to make it more transparent, in Appendix B we discuss an explicitly solvable toy model which
 625 mimics relevant features of the scalar Yukawa model in the three-body truncation. This illustrates our conclusions in
 626 a very simple and clear manner.

627 Within the three-body truncation, all calculated observables are expressed through the renormalized two-body Fock
 628 component found for $p^2 = m^2$, while the fully off-shell two-body Fock component $\Gamma_2^{(3)j}(k_\perp, x; p^2)$ with $p^2 \neq m^2$ is
 629 not needed for this purpose. Thus, it may seem that a set of critical constants $\alpha_c^{\text{off}}(p^2)$ is a sort of peculiarity having
 630 no relation to practical computations of physical quantities, while all actual restrictions imposed on the value of the
 631 coupling constant reduces to the requirement $\alpha \leq \alpha_c$. The importance of the function $\Gamma_2^{(3)j}(k_\perp, x; p^2)$ becomes evident
 632 as one goes to the four-body truncation, where the former enters, as an internal block, into the system of equations
 633 for the Fock components [8]. In this sense, the fully off-shell two-body vertex function serves as a “bridge” between
 634 the three- and four-body truncations. Respectively, the critical coupling constants $\alpha_c^{\text{off}}(p^2)$ propagate, together with
 635 $\Gamma_2^{(3)j}(k_\perp, x; p^2)$, to the four-body problem as well. The parameter p^2 in the four-body truncation varies continuously
 636 from $-\infty$ up to $(m - \mu)^2$. Our computations for $m = 0.94$, $\mu = 0.14$, and an infinite PV mass μ_1 show that $\alpha_c^{\text{off}}(p^2)$
 637 is a decreasing function of p^2 . It reaches its minimal value at the maximal available p^2 , i.e., $p^2 = (m - \mu)^2$. Hence, in
 638 the four-body truncation, one may expect the critical coupling constant to be not greater than $\alpha_c^{\text{off}}((m - \mu)^2) \simeq 2.382$.
 639 At the same time, one cannot exclude the possibility of appearance of a new, purely “four-body”, critical coupling
 640 constant. Numerical estimations [8, 9] based on an iterative procedure show that the iterations stop converging at
 641 α about 2.14 or larger. Exact calculation of the critical coupling constant in the four-body truncation however goes
 642 beyond the scope of the present paper. The above example with the hierarchy of the critical coupling constants is
 643 given to demonstrate that some of them originated from a given order truncation as mathematical peculiarities may
 644 then propagate to higher order truncations and then introduce further physical restrictions on the parameters of the
 645 model.

646 VII. CALCULATION OF THE ELECTROMAGNETIC FORM FACTOR

647 Form factors are fundamental for the study of hadron structures. They are defined from the electromagnetic vertex
 648 (EMV) $G^\rho(p, p')$ which is expressed through the matrix element of the current operator $\hat{J}_{\text{em}}^\rho(x)$:

$$G^\rho(p, p') = e_0 \langle p' | \hat{J}_{\text{em}}^\rho(0) | p \rangle, \quad (109)$$

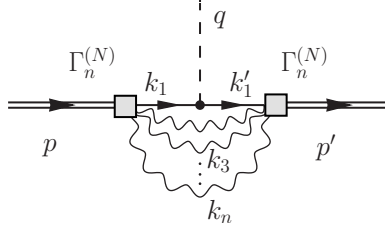


FIG. 13. n -body electromagnetic vertex in the truncation of order N . The dashed line corresponds to a photon. The nucleon-photon interaction vertex is given by $e_{0(N-n+1)}(k_1 + k'_1)^\rho$.

649 where p and p' are the initial and final particle four-momenta, e_0 is the bare electromagnetic coupling constant, and
 650 ρ is an arbitrary Lorentz index. The bra and ket vectors here are the same as the state vectors $\phi^\dagger(p')$ and $\phi(p)$,
 651 respectively. The elastic electromagnetic form factor $F(Q^2)$ for a scalar particle is defined as

$$G^\rho(p, p') = e(p + p')^\rho F(Q^2), \quad (110)$$

652 where e is the physical electromagnetic coupling constant (physical charge), $Q^2 = -q^2$, $q = p' - p$ is the four-
 653 momentum transfer. The necessity to distinguish the physical and bare electromagnetic coupling constants follows
 654 from the fact that the elementary electromagnetic vertex, generally speaking, is renormalized due to its “dressing” by
 655 scalar pion lines. The standard renormalization condition known from QED demands that the renormalized EMV at
 656 zero momentum transfer must coincide with that for the free particle:

$$G^\rho(p, p) = 2ep^\rho. \quad (111)$$

657 This condition yields a relation between e_0 and e .

658 The structure of the EMV (110) is a consequence of general physical symmetries of the interaction. In approximate
 659 nonperturbative calculations in the framework of LFD these symmetries may be broken because of the rotational
 660 symmetry violation. This fact may lead to appearance, in the EMV, of nonphysical contributions explicitly depending
 661 on the light front orientation [18]. In the spinless case the problem is however absent for the plus-component of the
 662 EMV, provided an additional requirement $q^+ = 0$ is imposed on the momentum transfer. After that, the form factor
 663 can be expressed through the EMV by

$$eF(Q^2) = \frac{G^+(p, p')}{2p^+}. \quad (112)$$

664 The renormalization condition (111) is implied to refer to the plus-component of the EMV as well. With Eq. (112),
 665 it can be written in a very simple form

$$F(0) = 1. \quad (113)$$

With the Fock representation of the state vector in N -body truncated Fock space, the total EMV is a sum of n -body contributions ($n = 1, 2, \dots, N$) shown in Fig. 13. According to the FSDR rules, the bare electromagnetic coupling constant e_0 must be a sector-dependent quantity

$$e_0 \rightarrow e_{0l}, \quad (l = 1, 2, \dots, N),$$

666 similar to the bare coupling constant g_0 which determines the interaction between the constituents of the state vector
 667 [see Eq. (29)]. However, in contrast to g_0 treated nonperturbatively, e_0 is considered as being small, so that the EMV
 668 is calculated in the leading order in e_0 (at the same time, the renormalization of e_0 due to its “dressing” by scalar
 669 pion lines is nonperturbative!). Then, since e_0 has no relation to the interactions “inside” the state vector, we will
 670 refer to it as an external bare coupling constant [6]. Now the photon as an external particle should be excluded from
 671 the particle counting, and the Fock sector content is fully determined by the number of scalar pion-spectators plus
 672 one scalar nucleon. We thus have the following rule to calculate the index l for the n -body Fock sector: $l = N - n_s$,
 673 where $n_s = n - 1$ is the number of pion-spectators. The lowest order external bare coupling constant $e_{01} = e$, because
 674 the trivial case $N = 1$ describes the interaction of a photon with a point-like scalar nucleon.

676 Applying the LFD graph techniques rules to the diagram in Fig. 13 and using Eq. (110), we obtain for the form
677 factor within the N -body Fock space truncation:

$$eF^{(N)}(Q^2) = \sum_{n=1}^N e_{0(N-n+1)} F_n^{(N)}(Q^2), \quad (114)$$

678 where

$$F_n^{(N)}(Q^2) = \frac{2}{(2\pi)^{3(n-1)}(n-1)!} \int \prod_{i=1}^n \frac{d^2 k_{i\perp} dx_i}{2x_i} \\ \times \left[\frac{\Gamma_n^{(N)}(\mathbf{k}_{2\perp}, x_2, \dots, \mathbf{k}_{n\perp}, x_n) \Gamma_n^{(N)}(\mathbf{k}'_{2\perp}, x_2, \dots, \mathbf{k}'_{n\perp}, x_n)}{(s_n - m^2)(s'_n - m^2)} \right] \delta^{(2)}\left(\sum_{i=1}^n \mathbf{k}_{i\perp}\right) \delta\left(\sum_{i=1}^n x_i - 1\right). \quad (115)$$

The primed transverse momenta are defined as

$$\mathbf{k}'_{i\perp} = \mathbf{k}_{i\perp} - x_i \mathbf{q}_\perp,$$

679 s'_n is given by Eq. (27), changing $\mathbf{k}_{i\perp}$ by $\mathbf{k}'_{i\perp}$. Note that, due to the condition $q^+ = 0$, we have $Q^2 = q_\perp^2$. Comparison
680 of Eqs. (115) and (40) gives

$$F_n^{(N)}(0) = I_n^{(N)}, \quad (116)$$

681 i.e., the n -body contribution to the form factor at zero momentum transfer coincides with the n -body Fock sector
682 norm. Setting $Q^2 = 0$ in Eq. (114) and making use of the renormalization condition (113) which writes simply
683 $F^{(N)}(0) = 1$ in truncated Fock space, we get

$$e = \sum_{n=1}^N e_{0(N-n+1)} I_n^{(N)}. \quad (117)$$

684 This formula, together with the normalization condition (39) leads to the following result:

$$e_{0l} = e \quad (118)$$

685 for arbitrary l . So, the electromagnetic coupling constant in the framework of FSDR is not renormalized at all.
686 Eq. (114) now becomes

$$F^{(N)}(Q^2) = \sum_{n=1}^N F_n^{(N)}(Q^2). \quad (119)$$

687 The one-body contribution is

$$F_1^{(N)}(Q^2) = \left[\psi_1^{(N)} \right]^2 = I_1^{(N)} = 1 - \sum_{n=2}^N I_n^{(N)}. \quad (120)$$

688 It does not depend on Q^2 . With Eq. (116), the final expression for the form factor reads

$$F^{(N)}(Q^2) = 1 + \sum_{n=2}^N \left[F_n^{(N)}(Q^2) - F_n^{(N)}(0) \right]. \quad (121)$$

689 Note that the general formula (115) for the n -body Fock sector contribution to the form factor does not take into
690 account PV particles, since the corresponding integrals do not need regularization in the scalar Yukawa model without
691 antiparticles. One may thus consider Eq. (115) to be related to the limiting case $\mu_1 \rightarrow \infty$.

692 In the two-body truncation the form factor is

$$F^{(2)}(Q^2) = 1 + F_2^{(2)}(Q^2) - F_2^{(2)}(0). \quad (122)$$

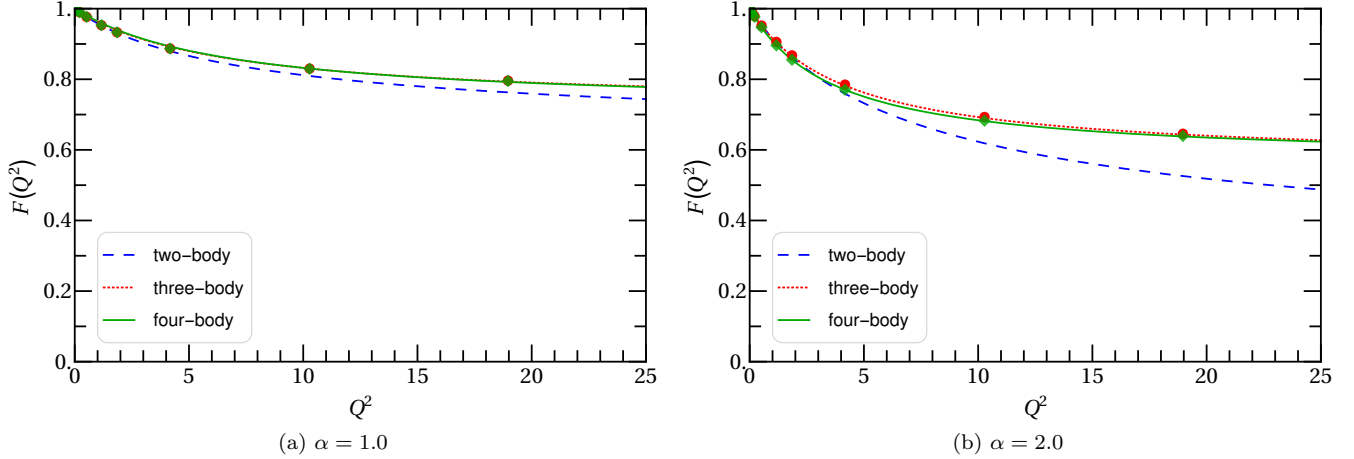


FIG. 14. Electromagnetic form factor calculated in the two-, three- and four-body truncations for $\alpha = 1.0$ (left panel) and $\alpha = 2.0$ (right panel), at $m = 0.94$, $\mu = 0.14$, and $\mu_1 = 15$. The results for the four-body truncation are adopted from Ref. [9]. The form factor in the two-body truncation admits an analytic expression. For the three- and four-body truncations, the obtained results (symbols) are fitted to a function (lines) $f(Q^2) = I_1 + (1 - I_1)/(1 + c_1 Q^2)/(1 + c_2 Q^2)$, where c_1 and c_2 are some constants depending on α and on the order of truncation.

693 Substituting the solution (51) into Eq. (115) for $n = N = 2$, we arrive at

$$F_2^{(2)}(Q^2) = \frac{g^2}{16\pi^3} \int_0^1 dx x(1-x) \int \frac{d^2 k_\perp}{[k_\perp^2 + \mu^2(1-x) + m^2 x^2][(\mathbf{k}_\perp - x\mathbf{q}_\perp)^2 + \mu^2(1-x) + m^2 x^2]}. \quad (123)$$

694 The integrals can be expressed in terms of elementary functions. It is interesting to note that the formulas (122)
 695 and (123) exactly reproduce the familiar perturbative result, though our approach does not rely on perturbation
 696 theory. This rather surprising fact can be explained by the simplicity of the two-body approximation. Already in the
 697 three-body truncation both two- and three-body vertex functions have rather complex dependence on the physical
 698 coupling constant, determined by Eqs. (77) and (64).

699 The form factor $F^{(N)}(Q^2)$ calculated numerically for $N = 2$, $N = 3$, and $N = 4$ is shown in Fig. 14. The calculations
 700 were carried out for $m = 0.94$, $\mu = 0.14$, $\mu_1 = 15$, and two different values of the coupling constant: $\alpha = 1.0$ and
 701 $\alpha = 2.0$. Here we retain a finite PV mass in the two- and three-body truncations in order to compare with the
 702 results in the four-body truncation obtained with the same PV mass [9]. This value of μ_1 is large enough to make the
 703 calculated results almost insensitive (in the scale of the plots) to its further increase. In principle, in the three-body
 704 truncation, one might take a bigger α , up to $\alpha_c \simeq 2.630$, inclusive. However, keeping in mind stronger limitations on
 705 the coupling constant in the four-body truncation (see the end of Sec. VIC), we took a lower value of α , in order
 706 to have the possibility to compare with each other the results for the form factor, obtained in the successive $N = 2$,
 707 $N = 3$, and $N = 4$ truncations.

708 Note that the functions $F_n^{(N)}(Q^2)$, Eq. (115), with $n \geq 2$ fall rapidly in the asymptotic region $Q^2 \gg \{m, \mu\}$ and
 709 tend to zero if $Q^2 \rightarrow \infty$. The limiting value of the form factor thus coincides with the one-body Fock sector norm:

$$F^{(N)}(Q^2 \rightarrow \infty) = I_1^{(N)}, \quad (124)$$

710 that is, generally speaking, a finite nonzero quantity.

711 VIII. DISCUSSION FOR THE x -DEPENDENCE OF $g_{03}(x)$

712 The x -dependent bare coupling constant $g_{03}(x)$ was introduced in Ref. [7]. This x -dependence which, at first glance,
 713 seems to be an oddity, is a consequence of truncation. As it was already mentioned, by truncating Fock space, we
 714 replace the initial light-front Hamiltonian (12) by a finite matrix. Finding, with this finite matrix, the vertex function

715 $\Gamma_2^{(N)}(k_\perp, x)$ and solving the renormalization condition (42) relative to g_{0N} , we find that the latter becomes dependent
716 on x : $g_{0N} = g_{0N}(x)$ [see Eq. (82) for the $N = 3$ case].

717 More precisely, the mechanism for the appearance of the x -dependent $g_{0N}(x)$ is the following. The renormalization
718 condition (42) contains the vertex function $\Gamma_2^{(N)}(k_\perp, x)$ calculated in N -body truncated Fock space and dependent on
719 the two kinematical variables k_\perp and x . The on-energy-shell condition $s_2 = m^2$ does not fix both variables, but gives
720 a relation between them. We express from this relation the value $k_\perp = k_\perp^*(x)$ which is given by Eq. (35). So, the value
721 of the vertex function which appears on the left-hand side of the renormalization condition (42) is $\Gamma_2^{(N)}(k_\perp^*(x), x)$, i.e.,
722 it depends on x via $k_\perp^*(x)$ and also via its “own” argument x . Since the right-hand side of Eq. (42) is a constant, this
723 condition can be satisfied identically only if the bare coupling constant g_{0N} , which the two-body vertex depends on,
724 becomes a function of x as well.

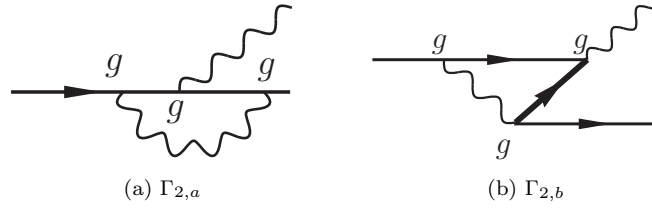


FIG. 15. Full set of perturbative contributions to the two-body vertex function at order $O(g^3)$. The thinner straight lines represent the scalar nucleon. The thicker straight line represents the antinucleon. The wavy lines represent the scalar pions.

725 As discussed in Sec. IV, the x -dependence of the on-energy-shell two-body vertex function must disappear, if the
726 latter was calculated in full (i.e., not truncated) Fock space. This general property is based on fundamental physical
727 symmetries. To illustrate how the cancellation of x -dependence happens in practice, within LFD, there is no need to
728 perform nonperturbative calculations of $\Gamma_2^{(N)}(k_\perp^*(x), x)$ involving contributions from all possible Fock sectors (i.e., for
729 $N \rightarrow \infty$). One may use the perturbative expansion of the two-body vertex function, which can be written as

$$\Gamma_2^{(N \rightarrow \infty)}(k_\perp^*(x), x) = \sum_{n=1}^{\infty} g^n \Gamma_2^{(g^n)}(k_\perp^*(x), x). \quad (125)$$

730 If $\Gamma_2^{(N \rightarrow \infty)}(k_\perp^*(x), x) = \text{const}$, then any coefficient $\Gamma_2^{(g^n)}(k_\perp^*(x), x)$ of the perturbation series is also x -independent.
731 We emphasize that $\Gamma_2^{(g^n)}$ involves contributions from all possible Fock sectors at order g^n of perturbation theory.

732 The simplest nontrivial case is the third order of perturbation theory. All the contributions to $\Gamma_2^{(g^3)}(k_\perp^*(x), x)$ are
733 exhausted by the two shown in Fig. 15. The graph (a) generated by the three-body Fock sector (one scalar nucleon
734 plus two scalar pions) represents a contribution incorporated in our nonperturbative three-body calculations of $\Gamma_2^{(3)}$
735 in Sec. VIA. The graph (b) represents a contribution from another three-body Fock sector (one scalar nucleon plus
736 one nucleon-antinucleon pair), which was omitted in the truncation we used. Below we will demonstrate that the full
737 $\Gamma_2^{(g^3)}(k_\perp^*(x), x)$, determined by the sum of two contributions (a) and (b), is indeed a constant with respect to x .

738 The amplitude of the diagram in Fig. 15(a) reads

$$\Gamma_{2,a}^{(g^3)}(k_\perp, x) = \frac{g^3}{(2\pi)^3} \int_0^{1-x} \frac{dx'}{2x'(1-x')(1-x-x')} \int \frac{d^2 k'_\perp}{(s'_2 - m^2)(s_3 - m^2)}. \quad (126)$$

741 The amplitude of the diagram in Fig. 15(b) reads

$$\Gamma_{2,b}^{(g^3)}(k_\perp, x) = \frac{g^3}{(2\pi)^3} \int_{1-x}^1 \frac{dx'}{2x'(1-x')(x+x'-1)} \int \frac{d^2 k'_\perp}{(s'_2 - m^2)(\bar{s}_3 - m^2)}. \quad (127)$$

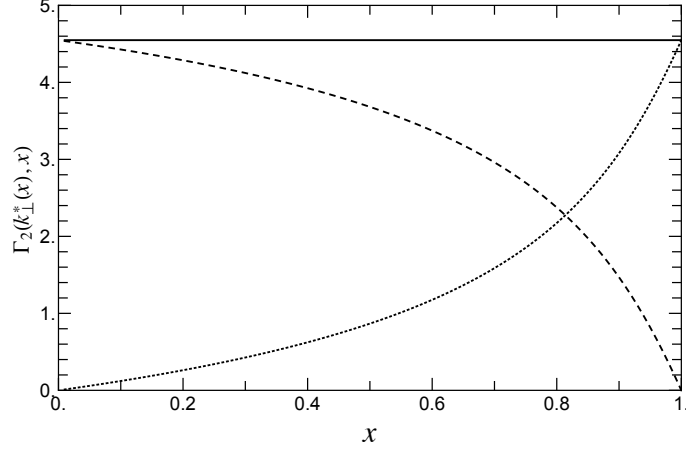


FIG. 16. Dependence of the on-energy-shell two-body vertex function in the g^3 -order of perturbation theory on the kinematical variable x . The dashed curve is $\Gamma_{2,a}^{(g^3)}(k_{\perp}^*(x), x)$, Fig. 15(a); the dotted curve is $\Gamma_{2,b}^{(g^3)}(k_{\perp}^*(x), x)$, Fig. 15(b); the solid curve represents their sum which is a constant.

742 The quantities s'_2 and s_3 defined by Eqs. (34), changing $k_{\perp} \rightarrow k'_{\perp}$, $x \rightarrow x'$, and (65) with $j = j' = 0$, respectively,
 743 are the invariant mass squared of each of the intermediate states of Fig. 15(a): nucleon plus pion and nucleon plus
 744 two pions. The quantity \bar{s}_3 is the invariant mass squared of the three-body state of Fig. 15(b), i.e., the nucleon plus
 745 nucleon-antinucleon pair:

$$\bar{s}_3 = \frac{k_{\perp}^2 + m^2}{1-x} + \frac{k'^2_{\perp} + m^2}{1-x'} + \frac{(\mathbf{k}_{\perp} + \mathbf{k}'_{\perp})^2 + m^2}{x+x'-1}. \quad (128)$$

746 Since each of the amplitudes (126) and (127) converge, we omit the PV particle contributions. To calculate the
 747 integrals, it is convenient to use the Feynman parametrization:

$$\frac{1}{ab} = \int_0^1 \frac{dv}{[va + (1-v)b]^2}. \quad (129)$$

748
 749 Then both integrals over $d^2k'_{\perp}$ can be calculated analytically. The integrals over dv are also calculated analytically.
 750 We substitute $k_{\perp} = k_{\perp}^*(x)$ with the imaginary value $k_{\perp}^*(x)$ from Eq. (35) and calculate the residual one-dimensional
 751 integrals over dx' numerically.

The calculated results are shown in Fig. 16. The dashed curve is $\Gamma_{2,a}^{(g^3)}(k_{\perp}^*(x), x)$, the contribution shown in Fig. 15(a). It depends on x . This x -dependence generates the x -dependence of $g_{03}(x)$, Eq. (82). The dotted curve is $\Gamma_{2,b}^{(g^3)}(k_{\perp}^*(x), x)$, the contribution shown in Fig. 15(b). It also depends on x . The solid line is the sum

$$\Gamma_2^{(g^3)}(k_{\perp}^*(x), x) = \Gamma_{2,a}^{(g^3)}(k_{\perp}^*(x), x) + \Gamma_{2,b}^{(g^3)}(k_{\perp}^*(x), x).$$

752 It does not depend on x . In the Yukawa model with spin, also in the perturbative framework, the same result was
 753 found in Ref. [7].

754 This example clearly shows that the origin of the x -dependence of the bare coupling constant $g_{03}(x)$ is the Fock
 755 space truncation. Taking into account the previously omitted contribution with an antinucleon we restore the constant
 756 value of g_{03} .

757 In principle, antiparticle degrees of freedom can be included into Fock space within the nonperturbative approach
 758 based on FSDR. This was done in Refs. [17] (within the scalar Yukawa model) and [7] (within the spinor Yukawa model
 759 in the quenched approximation, i.e., neglecting fermion-antifermion loop contributions). The results of numerical
 760 nonperturbative calculations of the on-energy-shell two-body vertex function $\Gamma_2^{(3)}(k_{\perp}^*(x), x)$ or the bare coupling
 761 constant $g_{03}(x)$ in the three-body truncation with the nucleon-nucleon-antinucleon Fock sector included show that
 762 the latter makes the x -dependence of the calculated quantities much weaker, even for rather large coupling constant
 763 values.

IX. CONCLUSION

764

765 With the interaction Hamiltonian $\mathcal{H}_{\text{int}}(x) = -g\chi^\dagger\chi\varphi$, where χ and φ are spinless fields referred as a “scalar
766 nucleon” and “scalar pion”, respectively, in the framework of light-front dynamics, we found nonperturbatively the
767 Fock components of the state vector in truncated Fock space including one-body (χ), two-body ($\chi+\varphi$), and three-body
768 ($\chi+2\varphi$) states (Fock sectors). The sector dependent renormalization of the coupling constant and the scalar nucleon
769 mass was used. In this transparent example, we exposed the general principles of nonperturbative renormalization
770 in truncated Fock space and demonstrated, by practical application, the main steps required to solve the problem.
771 The procedure contains the principal ingredients of more general applications, and, especially, the main features
772 of the sector dependent renormalization – appearance of the sector dependent renormalization parameters, i.e., the
773 bare coupling constants like g_{02} , g_{03} and the mass counterterms like δm_2^2 , δm_3^2 , related to different Fock sectors,
774 simultaneously in one system of equations for the Fock components. Though the constant g_{03} is not a true constant
775 – it depends on the kinematical variable x , – this and other constants do not contain any uncertainties and are found
776 unambiguously.

777 The case of the true Yukawa model (or other field theories), incorporating spin, differs from the example considered
778 here by technical details only (the form of propagators, the spin structure of the wave functions, etc.), but contains
779 the same steps. The case of higher order truncation is more complicated technically, since it requires the solution of
780 a more complicated system of equations, but it uses the same solution procedure.

781 This work presents the detailed theoretical framework that underlines the successful solution of the scalar Yukawa
782 model in four-body truncation when the ($\chi+3\varphi$) Fock sector is added to the three listed above [8, 9]. Comparison of
783 results in the three-body truncation with those in four-body truncation [8, 9] shows that convergence with respect to
784 the number of Fock sectors involved is achieved.

785

ACKNOWLEDGMENTS

786 The authors thank P. Maris for valuable remarks and constructive criticisms. One of the authors (V.A.K.) thanks the
787 Nuclear Theory Group at Iowa State University, where a part of this paper was prepared, for kind hospitality during
788 his visits. This work was supported in part by the Department of Energy under Grant Nos. DE-FG02-87ER40371
789 and DESC0008485 (SciDAC-3/NUCLEI). Computational resources were provided by the National Energy Research
790 Supercomputer Center (NERSC), which is supported by the Office of Science of the U.S. Department of Energy under
791 Contract No. DE-AC02-05CH11231.

792

Appendix A: Two-body self-energy

793 The two-body scalar nucleon self-energy is given by Eq. (48) which can be written as

$$\bar{\Sigma}^{(2)}(p^2) = -\frac{1}{16\pi^2} \sum_{j=0}^1 (-1)^j \int_0^1 dx \int_0^\infty \frac{dk_\perp^2}{k_\perp^2 + \mu_j^2(1-x) + m^2x - p^2x(1-x)}. \quad (\text{A1})$$

794 Without PV regularization, the integral over dk_\perp^2 diverges logarithmically at the upper limit. It is convenient to define
795 the regular function

$$a(p^2, m_1, m_2) \equiv \int_0^1 dx \int_0^\infty dk_\perp^2 \left[\frac{1}{k_\perp^2 + m_1^2(1-x) + m_2^2x - p^2x(1-x)} - \frac{1}{k_\perp^2 + m^2} \right]. \quad (\text{A2})$$

796 Then

$$\bar{\Sigma}^{(2)}(p^2) = -\frac{1}{16\pi^2} [a(p^2, \mu, m) - a(p^2, \mu_1, m)]. \quad (\text{A3})$$

The integrals in Eq. (A2) are easily calculated. We introduce the notation

$$D \equiv p^4 - 2(m_1^2 + m_2^2)p^2 + (m_1^2 - m_2^2)^2.$$

797 Then

$$a(p^2, m_1, m_2) = 2 - \log \frac{m_1 m_2}{m^2} + \frac{m_1^2 - m_2^2}{p^2} \log \frac{m_2}{m_1} + \frac{\sqrt{|D|}}{p^2} \Phi(p^2, m_1, m_2), \quad (\text{A4})$$

798 where

$$\Phi(p^2, m_1, m_2) = \begin{cases} \log \left(\frac{m_1^2 + m_2^2 - p^2 + \sqrt{D}}{2m_1 m_2} \right), & \text{if } D \geq 0, \\ -\arctan \left(\frac{\sqrt{|D|}}{m_1^2 + m_2^2 - p^2} \right), & \text{if } D < 0. \end{cases} \quad (\text{A5})$$

799 The function $a(p^2, m_1, m_2)$ is symmetric with respect to the permutation of m_1 and m_2 . At $p^2 < (m_1 + m_2)^2$ it is
800 real.

801 In the limit of infinite PV mass μ_1 the difference $\bar{\Sigma}_c^{(2)}(p^2) = \bar{\Sigma}^{(2)}(p^2) - \bar{\Sigma}^{(2)}(m^2)$ tends to a finite value:

$$\bar{\Sigma}_c^{(2)}(p^2) = -\frac{1}{16\pi^2} [a(p^2, \mu, m) - a(m^2, \mu, m)]. \quad (\text{A6})$$

802 At $p^2 \rightarrow -\infty$ we get the following asymptotic behavior:

$$\bar{\Sigma}_c^{(2)}(p^2) \approx \frac{1}{16\pi^2} \log \frac{|p^2|}{m^2} + \dots, \quad (\text{A7})$$

803 where the dots designate finite terms.

In contrast to the self-energy, its derivative over p^2 does not need regularization, so, $\bar{\Sigma}^{(2)'}(m^2)$ is finite in the limit of infinite PV mass. Its limiting value is calculated as

$$\bar{\Sigma}_c^{(2)'}(m^2) = -\frac{1}{16\pi^2} \left. \frac{\partial a(p^2, \mu, m)}{\partial p^2} \right|_{p^2=m^2}.$$

804 The calculation of the derivative is straightforward. It yields

$$\bar{\Sigma}_c^{(2)'}(m^2) = -\frac{1}{16\pi^2 m^2} \left[\frac{\xi(3 - \xi^2)}{\sqrt{4 - \xi^2}} \arctan \left(\frac{\sqrt{4 - \xi^2}}{\xi} \right) - 1 + (1 - \xi^2) \log \frac{1}{\xi} \right], \quad (\text{A8})$$

805 where $\xi = \mu/m$. Eq. (A8) is valid for $\mu < 2m$.

806

Appendix B: Critical coupling constant in explicitly solvable model

807 In this section we consider, as an illustration, an explicitly solvable model which reflects all important properties of
808 Eqs. (70), (77), and (85), related to the existence of the critical coupling constant. We will not analyze the ‘‘Landau
809 pole’’ type critical coupling constant (60) caused by the two-body self-energy contribution but, instead, focus on the
810 critical coupling originating from the kernel of the integral term in each of the equations discussed. According to the
811 terminology of Sec. VI C, we are interested in the critical coupling constant coming from the discrete eigenvalue λ_0
812 which strongly depends on the particular form of the integration kernel.

813 Each of the equations is a Fredholm integral equation of the second kind, which can be written schematically in
814 the form (88). The integral operator \hat{A} depends on the coupling constant α . The critical coupling constant α_c is a
815 solution of the matrix equation $\det(\hat{A} - \mathbb{I}) = 0$, where \mathbb{I} is a unity matrix. If $\alpha = \alpha_c$, the solution Γ_2 as a function of
816 α becomes singular: it has a pole $\sim 1/(\alpha - \alpha_c)$.

817 Let us first summarize what is already known about, concerning the critical coupling in the equations mentioned
818 above. The equation (70) for the nonrenormalized $\Gamma_2^{(3)j}(k_\perp, x)$, where the inhomogeneous part $g_{03}\psi_1^{(3)}[1 - g^2\bar{I}_2^{(2)}]$ is
819 treated as an independent quantity (a constant or a function of x), has a critical coupling constant. For the physical
820 particle masses $m = 0.94$, $\mu = 0.14$, and an infinite PV mass μ_1 its value is $\alpha_c^{\text{nr}} \simeq 2.190$. After the renormalization
821 leading to Eq. (77), this critical coupling disappears, i.e., the renormalized $\Gamma_2^{(3)j}(k_\perp, x)$ is smooth at $\alpha = \alpha_c^{\text{nr}}$. We see

822 that the role of renormalization in deleting infinities is two-fold: the renormalization not only deletes field theoretical
 823 divergences (e.g., the logarithmic ultraviolet divergence in the two-body self-energy $\Sigma^{(2)}$), but also removes the pole
 824 singularity of the Fock components at $\alpha = \alpha_c^{\text{nr}}$. In the generalized equation (85) for the fully off-shell two-body vertex
 825 function $\Gamma_2^{(3)j}(k_\perp, x; p^2)$ the critical coupling constant arises again, now as a function of p^2 . We will show that all
 826 these properties can be easily traced and explained by using a toy model which admits analytic solution.

827 We start with the equation

$$F(k, x) = g_0(x)\psi_1 + \int K(k, x, k', x')F(k', x')dk'dx' \quad (\text{B1})$$

828 with the separable kernel

$$K(k, x, k', x') = \alpha h(k, x)h(k', x'). \quad (\text{B2})$$

829 Here F is an unknown function to be found, g_0 and h are smooth bounded functions of their arguments, and ψ_1 is a
 830 constant. We do not specify the limits of integration, assuming that all integrals hereafter are convergent (e.g., due to
 831 proper regularization). Eq. (B1) is an analog of the equation (70) for the nonrenormalized two-body vertex function.
 832 Its solution is easily found and has the form

$$F(k, x) = g_0(x)\psi_1 + \frac{\alpha h(k, x)}{1 - \frac{\alpha}{\alpha_c}} \int h(k', x')g_0(x')\psi_1 dk'dx', \quad (\text{B3})$$

833 where

$$\frac{1}{\alpha_c} = \int h^2(k', x')dk'dx'. \quad (\text{B4})$$

834 It is seen that $F(k, x)$ is singular at $\alpha = \alpha_c$. The latter quantity is a full analog of the critical coupling constant α_c^{nr}
 835 (see Sec. VIC).

836 Now we apply a “renormalization” procedure to the function $F(k, x)$. In the Yukawa model we imposed the
 837 renormalization condition on the function $\Gamma_2^{(N)}(k_\perp, x)$ at $s_2 = m^2$ which corresponds to an x -dependent point $k_\perp =$
 838 $k_\perp^*(x)$ given by Eq. (35). We will keep this analogy and impose the renormalization condition on $F(k, x)$ in some
 839 point $k = k^*(x)$:

$$F(k^*(x), x) = g \quad (\text{B5})$$

840 and demand its fulfillment for all values of x . Now the function $g_0(x)$ can not be considered as being fixed *a priori*
 841 and should be found along with the renormalized $F(k, x)$. Substituting $F(k, x)$ from Eq. (B3) into Eq. (B5), we get

$$g_0(x)\psi_1 + \frac{\alpha h(k^*(x), x)}{1 - \frac{\alpha}{\alpha_c}} \int h(k', x')g_0(x')\psi_1 dk'dx' = g. \quad (\text{B6})$$

843 This equation is easily solved relative to $g_0(x)$. After that, we find the relation between the “bare” (x -dependent)
 844 coupling constant $g_0(x)$ and the “physical” one, g :

$$g_0(x)\psi_1 = g \left(\frac{1 - \frac{\alpha}{\alpha_c} + \alpha \int [h(k^*(x'), x') - h(k^*(x), x)] h(k', x') dk'dx'}{1 - \frac{\alpha}{\alpha_c} + \alpha \int h(k^*(x'), x') h(k', x') dk'dx'} \right). \quad (\text{B7})$$

846 Substituting this expression for $g_0(x)\psi_1$ into Eq. (B3), we obtain the renormalized solution

$$F(k, x) = g + \frac{g\alpha[h(k, x) - h(k^*(x), x)] \int h(k', x') dk'dx'}{1 - \frac{\alpha}{\alpha_c} + \alpha \int h(k^*(x'), x') h(k', x') dk'dx'}. \quad (\text{B8})$$

848 It satisfies the equation

$$F(k, x) = g + \int [K(k, x, k', x') - K(k^*(x), x, k', x')] F(k', x') dk'dx' \quad (\text{B9})$$

849 analogous to the equation (77) for the renormalized two-body vertex function. Note that after the renormalization
 850 $F(k, x)$ has no any singularity at $\alpha = \alpha_c$.

851 The mechanism for the removal of the singularity at $\alpha = \alpha_c$ is nontrivial, since it is not reduced to the cancellation
 852 of factors like $(\alpha - \alpha_c)$. Such a cancellation would take place if $g_0(x)$ did not depend on x . To explain this point,
 853 consider, for a moment, another form of the renormalization condition, as compared to Eq. (B5). Namely, we impose
 854 it not for all values of x simultaneously, but for a particular value $x = x^*$ only: $F(k^*(x^*), x^*) = g$. Now, expressing
 855 the product $g_0\psi_1$ via α , we obtain that the former is a true constant proportional to $(\alpha - \alpha_c)$. It cancels the $1/(\alpha - \alpha_c)$
 856 singularity of the nonrenormalized solution. At $\alpha = \alpha_c$ the inhomogeneous term vanishes and the renormalized $F(k, x)$
 857 becomes a solution of the homogeneous equation, which exists just at this critical value of α . After the x -dependence
 858 of $g_0(x)$ is taken into account (as it should be), the function $g_0(x)$ does not turn into zero at $\alpha = \alpha_c$, in contrast to the
 859 case $g_0(x) = \text{const}$. The cancellation of the singularity $1/(\alpha - \alpha_c)$ in Eq. (B3) takes place only after the calculation
 860 of the double integral. Due to this fact the renormalized solution becomes nonsingular and smooth at $\alpha = \alpha_c$.

861 It is also instructive to find the corresponding ‘‘off-shell’’ solution satisfying the equation [cf. with Eq. (B1)]:

$$F(k, x; p) = g_0(x)\psi_1(p) + \int K(k, x, k', x'; p)F(k', x'; p)dk'dx', \quad (\text{B10})$$

862 where

$$K(k, x, k', x'; p) = \alpha h(k, x; p)h(k', x'; p). \quad (\text{B11})$$

The ‘‘off-shell’’ continuation is given by the additional dependence of all parts of the equation on the parameter p .
 The ‘‘on-shell’’ equation, completely equivalent to Eq. (B1), is obtained at $p = m$. The renormalization condition is
 still imposed on the mass shell $p = m$:

$$F(k^*(x), x; m) = g,$$

863 whereas Eq. (B10) determines the solution $F(k, x; p)$ for arbitrary p . After the renormalization, Eq. (B10) becomes
 864 an analog of Eq. (85). Its solution can be found in a similar fashion to the on-shell solution (B8) and has the form

$$F(k, x; p) = g \frac{\psi_1(p)}{\psi_1(m)} \left\{ 1 - \alpha \frac{J_1(m)h(k^*(x), x; m)}{1 - \frac{\alpha}{\alpha_c(m)} + \alpha J_2(m)} + \alpha \left[\frac{1 - \frac{\alpha}{\alpha_c(m)}}{1 - \frac{\alpha}{\alpha_c(p)}} \right] \frac{J_1(p)h(k, x; m)}{1 - \frac{\alpha}{\alpha_c(m)} + \alpha J_2(m)} \right. \\ \left. + \alpha \left[\frac{J_1(p)J_2(m) - J_1(m)J_2(p)}{1 - \frac{\alpha}{\alpha_c(p)}} \right] \frac{h(k, x; p)}{1 - \frac{\alpha}{\alpha_c(m)} + \alpha J_2(m)} \right\}, \quad (\text{B12})$$

865 where

$$J_1(p) = \int h(k', x'; p)dk'dx', \\ J_2(p) = \int h(k', x'; p)h(k^*(x'), x'; m)dk'dx',$$

and

$$\frac{1}{\alpha_c(p)} = \int h^2(k', x'; p)dk'dx'.$$

866 A peculiarity of the solution (B12) consists in the fact that, in contrast to the on-shell renormalized solution (B8), it
 867 is singular at $\alpha = \alpha_c(p)$, in spite of renormalization. A similar peculiarity happens with the fully off-shell two-body
 868 vertex function $\Gamma_2^{(3)j}(k_\perp, x; p^2)$ which is singular at $\alpha = \alpha_c^{\text{off}}(p^2)$.

869 On the mass shell $p = m$, we find that

$$\left[\frac{1 - \frac{\alpha}{\alpha_c(m)}}{1 - \frac{\alpha}{\alpha_c(p)}} \right]_{p=m} \Rightarrow 1, \\ \left[\frac{J_1(p)J_2(m) - J_1(m)J_2(p)}{1 - \frac{\alpha}{\alpha_c(p)}} \right]_{p=m} \Rightarrow 0.$$

870 Then the solution (B12) coincides with the on-shell solution (B8) and it is nonsingular at $\alpha = \alpha_c(m)$.

871 It is interesting to trace how the singularity at $\alpha = \alpha_c(p)$ disappears, when $p \rightarrow m$. Extracting the pole term
872 $\sim [\alpha - \alpha_c(p)]^{-1}$ from Eq. (B12) in this limit, we get, up to terms of order $(p - m)$, inclusive:

$$F(k, x; p \rightarrow m) = c \cdot \frac{h(k, x; m)(p - m)}{\alpha - \alpha_c(p)} + \dots, \quad (\text{B13})$$

where

$$c = \frac{g \{ \alpha_c(m) [J_1(m) J_2'(m) - J_1'(m) J_2(m)] + \alpha_c'(m) J_1(m) \}}{J_2(m)},$$

873 the primes denote the corresponding derivatives and the dots designate all nonpole contributions. At $\alpha = \alpha_c(p)$ the
874 solution (B13) vs. α is singular for arbitrary $p \neq m$, though the residue at the pole reduces when p approaches m .
875 The singularity disappears only if p exactly equals m . So, the cancellation of the singularity in the on-shell solution
876 $F(k, x; m)$ happens due to subtle balance between different terms in the equation, caused by the renormalization.

877 The above analysis distinctly shows that there exists one-to-one correspondence between the properties of this toy
878 model and the scalar Yukawa model, concerning the behavior of their solutions as a function of the coupling constant.

879 Thus, in each of the two models

- 880 (i) the nonrenormalized solution has a pole at a certain (critical) value of the coupling constant $\alpha = \alpha_c$;
- 881 (ii) the singularity $1/(\alpha - \alpha_c)$ disappears after the renormalization and the renormalized solution is smooth at $\alpha = \alpha_c$;
- 882 (iii) both the ‘‘off-shell’’ solution like the two-body vertex $\Gamma_2^{(3)j}(k_\perp, x; p^2)$ introduced in Sec. VIB and the function
883 $F(k, x; p)$ satisfying Eq. (B10) are singular at some (critical) value of the coupling constant $\alpha = \alpha_c(p)$ depending on
884 the parameter p , even after renormalization;
- 885 (iv) the pole $1/[\alpha - \alpha_c(p)]$ of the ‘‘off-shell’’ solution exists for an arbitrary value of p , not equal to its on-mass-shell
886 value m , and disappears identically for $p = m$ only.

- 887 [1] R.J. Perry, A. Harindranath, and K.G. Wilson, Phys. Rev. Lett. **65**, 2959 (1990).
- 888 [2] P.A.M. Dirac, Rev. Mod. Phys. **21**, 392 (1949).
- 889 [3] J. Carbonell, B. Desplanques, V.A. Karmanov, and J.-F. Mathiot, Phys. Rep. **300**, 215 (1998).
- 890 [4] S.J. Brodsky, H. Pauli, and S.S. Pinsky, Phys. Rep. **301**, 299, (1998).
- 891 [5] F. Coester, Prog. Part. Nucl. Phys. **29**, 1 (1992).
- 892 [6] V.A. Karmanov, J.-F. Mathiot, and A.V. Smirnov, Phys. Rev. D **77**, 085028 (2008).
- 893 [7] V.A. Karmanov, J.-F. Mathiot, and A.V. Smirnov, Phys. Rev. D **86**, 085006 (2012).
- 894 [8] Y. Li, V.A. Karmanov, P. Maris, and J.P. Vary, Few-Body Syst. **56**, 495 (2015).
- 895 [9] Y. Li, V.A. Karmanov, P. Maris, and J.P. Vary, Phys. Lett. B **748**, 278 (2015).
- 896 [10] D. Bernard, Th. Cousin, V.A. Karmanov, and J.-F. Mathiot, Phys. Rev. D **65**, 025016 (2001).
- 897 [11] J.R. Hiller and S.J. Brodsky, Phys. Rev. D **59**, 016006 (1998).
- 898 [12] G. Baym, Phys. Rev. **117**, 886 (1960).
- 899 [13] F. Gross, Ç. Şavkli, and J. Tjon, Phys. Rev. D **64**, 076008, (2001).
- 900 [14] V.A. Karmanov, J.-F. Mathiot, and A.V. Smirnov, Phys. Rev. D **69**, 045009 (2004)
- 901 [15] M. E. Peskin and D. V. Schroeder, *An Introduction To Quantum Field Theory*, Addison-Wesley Advanced Book Program,
902 1995.
- 903 [16] V.A. Karmanov, J.-F. Mathiot, and A.V. Smirnov, Phys. Rev. D **82**, 056010 (2010).
- 904 [17] J.-F. Mathiot, A.V. Smirnov, N.A. Tsirova, and V.A. Karmanov, Few-Body Syst. **49**, 183 (2011).
- 905 [18] V.A. Karmanov and A.V. Smirnov, Nucl. Phys. **A546**, 691 (1992).